Amala
INSTITUTE OF MEDICAL SCIENCES
NABH ACCREDITED | ISO 9001: 2015

ISSN : 3050-5941
Online ISSN : 3050-595X

Volume 2 • Issue 1 • January-June 2025

Journal of Advanced Health Research and Clinical Medicine

An Official Publication of Amala Institute of Medical Sciences (AIMS)

https://journals.lww.com/hrcm

Wolters Kluwer

Medknow

P-ISSN: 3050-5941
E-ISSN: 3050-595X

Journal of Advanced Health Research & Clinical Medicine

Editorial Board

Journal of
Advanced Health Research & Clinical Medicine

Volume 2 ¦ Issue 1 ¦ January-June 2025

Contents

Tuberculosis Beyond Lungs: An Ancient but Unremitting Problem

"A dread disease in which the struggle between soul and body is so gradual, quiet and solemn and the result so sure that day by day and grain by grain, the mortal part wastes and withers away. A disease … which sometimes moves in giant strides and sometimes at a tardy sluggish pace, but, slow or quick, is ever sure and certain …"

Charles Dickens: Nicholas Nickleby

Since the beginning of time, tuberculosis (TB) has plagued humanity due to its significant social and economic impact on human existence on a global scale. Over 10 million new cases of TB are reported worldwide each year, affecting over 25% of the world's population.[1] Thirty high-burden nations account for 87% of all notified cases worldwide. Nearly 28% of all TB cases recorded worldwide are from India.[2] Pulmonary TB is the most common form of TB. Approximately 85% of TB cases that are reported globally involve the lungs.[3] TB can potentially infect organs other than the lungs, known as extrapulmonary TB (EPTB). There are several types of EPTB; some can be fatal, while others cause chronic illness and impairment that lowers quality of life.[4] There are still many difficulties in diagnosing and treating EPTB, despite the fact that we have made great strides in the diagnosis and management of pulmonary TB. Its involvement in nearly every bodily system and the lack of specificity surrounding clinical care has made it a foe in the fight against TB. Early clinical diagnosis of EPTB is hampered by its nonspecific clinical signs, which might mimic those of any other illness. Furthermore, the diagnosis of EPTB is frequently delayed because extra-pulmonary lesions are paucibacillary in nature and sample collection frequently necessitates invasive procedures. As a result, diagnosing and treating EPTB continues to be difficult in the quest to eradicate TB.[5] Hematogenous and lymphatic dispersion of *Mycobacterium tuberculosis* is the primary mechanism by which EPTB spreads.[6-9]

The country's socioeconomic status and the extent of TB control programs' execution have a significant impact on EPTB rates. Different populations have seen an increase in the percentage of EPTB among all reported TB cases. Although pulmonary TB could be controlled with the aid of numerous TB control initiatives, EPTB rates are not declining.[10] The ratio of EPTB to pulmonary TB cases in impoverished nations like India is 15%–20%. Among patients who also have HIV, this percentage rises to over 50%, indicating that the host's immune state is a significant risk factor for EPTB. The prevalence of EPTB varies by age and sex, indicating variations in host characteristics such as immunity.[11,12] The age bracket that is impacted by EPTB varies throughout studies; some reports link it to younger ages, while others link it to older ages. Male patients under 60 years old have been found to have both EPTB and pulmonary TB co-occurring, whereas female patients over 60 years old have isolated EPTB.[13] To determine if an EPTB case is contagious and to aid in diagnosis, all suspected cases must be evaluated for pulmonary TB also.[14] Research continuously demonstrates that pulmonary TB is more common in men, and EPTB is more common in women.[15] While tubercular pleural effusion is more common in men, tubercular lymphadenitis is more common in women. Young females (20–39 years old) were more likely to have genitourinary TB, while male adolescents were more likely to have central nervous system TB.[16] The most often affected site of EPTB is the lymph node, which is followed by the pleural cavity. It is interesting to note that TB of the bones and joints is more prevalent among EPTB cases in Taiwan (24.5%) and Russia (34.5%).[17]

Liver illness has been demonstrated to be a risk factor for peritoneal TB on its own, and the risk of disseminated disease was elevated by HIV co-infection and prior TB therapy. The infamous and fatal coinfection of HIV and TB led to a worldwide comeback of TB with the start of the HIV/AIDS epidemic in 1981. Numerous host genes were recognized to play a role in the spread of TB: In a case–control study, the Toll-like receptor 2 genotype T597C was linked to TB meningitis and exacerbated neurologic symptoms.[18] According to the same study, pleural TB was linked to genetic variations in interleukin. People who are homozygous with the interferon-gamma (+874) A allele are 3.75 times more likely to have TB.[19] Diabetes patients with EPTB had a high chance of dying, and TB reactivation appears to happen at least 4 years after the initial diabetes diagnosis.[20] Being the nation with the largest TB burden and having a high population of diabetics provide significant challenges for the healthcare system in India. An estimated 2.7 million incident TB cases occur in India.[21] Kerala, a state in south India with a population of 34.6 million, has a high prevalence of diabetes mellitus, with estimates ranging from 16% to 20%.[21] Because diabetes impairs immunity and pleural effusion is the most frequent location of EPTB involvement, diabetes raises the risk of acquiring TB by almost three times. Similarly, cancer patients have a 9–22 times higher risk of developing EPTB than the general population due to compromised immune systems.

Even with a cure and information on how to stop transmission, EPTB is still a major public health concern for a sizable section of the global population. While identifying EPTB is crucial for improving care, programs in underdeveloped nations tend

to address it less effectively than PTB. Examining EPTB determinants and identifying people at higher risk for EPTB is essential to improving TB treatment and the prognosis of the disease. Numerous factors, including co-morbidities, HIV coinfection, host factors, genetic variation, and the infection site, influence the spread of TB and the acquisition of EPTB type. The goal of TB treatment is to treat those who have active TB using standardized regimens and follow-up for drug resistance. To prevent the spread of the illness, treating people with active TB should be the top priority for TB control. However, identifying and treating those with latent TB should also be a top priority. Preventive therapy, clinical vigilance, public health initiatives, and health system improvement are all important components of the multi-level approach to EPTB prevention, especially for vulnerable and high-burden groups. Integration across HIV and immunosuppressive treatment programs is also required. Future studies are required to develop new biomarkers and tests that may improve the diagnosis of EPTB. Moreover, clinical suspicion is still necessary for precise identification.

Cherumadathil R. Saju

Department of Community Medicine, Amala Institute of Medical Sciences, Thrissur, Kerala, India

Address for correspondence: Dr. Cherumadathil R. Saju, Department of Community Medicine, Amala Institute of Medical Sciences, Amala Nagar, Thrissur - 680 555, Kerala, India.
E-mail: drsajucr@gmail.com

Received: 10-04-2025
Revised: 15-04-2025
Accepted: 16-04-2025
Published: ***

References

1. Singh R, Dwivedi SP, Gaharwar US, Meena R, Rajamani P, Prasad T. Recent updates on drug resistance in *Mycobacterium tuberculosis*. J Appl Microbiol 2020;128:1547-67.
2. Rolo M, González-Blanco B, Reyes CA, Rosillo N, López-Roa P. Epidemiology and factors associated with extra-pulmonary tuberculosis in a low-prevalence area. J Clin Tuberc Other Mycobact Dis 2023;32:100377.
3. World Health Organization. Global Tuberculosis Report 2022. World Health Organization; 2022. Available from: https://www.iris.who.int/bitstream/handle/10665/363752/9789240061729-eng.pdf?sequence=1. [Last accessed on 2025 Mar 05].
4. Sharma SK, Ryan H, Khaparde S, Sachdeva KS, Singh AD, Mohan A, *et al*. Index-TB guidelines: Guidelines on extrapulmonary tuberculosis for India. Indian J Med Res 2017;145:448-63.
5. Training Module on Extrapulmonary TB 2023 by Govt. of India. Available from: https://www. 7702334778Training_Module_on_Extrapulmonary_TB_-_Book_24032023.pdf. [Last accessed on 2025 Mar 05].
6. Moule MG, Cirillo JD. *Mycobacterium tuberculosis* dissemination plays a critical role in pathogenesis. Front Cell Infect Microbiol 2020;10:65.
7. Dunlap NE, Bass J, Fujiwara P, Hopewell P, Horsburgh Jr CR, Salfinger M, *et al*. Diagnostic Standards and Classification of Tuberculosis in Adults and Children. This official statement of the American Thoracic Society and the Centers for Disease Control and Prevention was adopted by the ATS Board of Directors, July 1999. This statement was endorsed by the Council of the Infectious Disease Society of America, September 1999. Am J Respir Crit Care Med 2000;161:1376-95.
8. Sharma SK, Mohan A. Miliary Tuberculosis. Microbiol Spectr 2017;5. [doi: 10.1128/microbiolspec].
9. Golden MP, Vikram HR. Extrapulmonary tuberculosis: An overview. Am Fam Physician 2005;72:1761-8.
10. Peto HM, Pratt RH, Harrington TA, LoBue PA, Armstrong LR. Epidemiology of extrapulmonary tuberculosis in the United States, 1993-2006. Clin Infect Dis 2009;49:1350-7.
11. TB Statistics for India; 2012. Available from: https://www.tbfacts.org/tb-statistics-india.html. [Last accessed on 2025 Mar 05].
12. Narain JP, Lo YR. Epidemiology of HIV-TB in Asia. Indian J Med Res 2004;120:277-89.
13. Kang W, Yu J, Du J, Yang S, Chen H, Liu J, *et al*. The epidemiology of extrapulmonary tuberculosis in China: A large-scale multi-center observational study. PLoS One 2020;15:e0237753.
14. Ohene SA, Bakker MI, Ojo J, Toonstra A, Awudi D, Klatser P. Extra-pulmonary tuberculosis: A retrospective study of patients in Accra, Ghana. PLoS One 2019;14:e0209650.
15. Sunnetcioglu A, Sunnetcioglu M, Binici I, Baran AI, Karahocagil MK, Saydan MR. Comparative analysis of pulmonary and extrapulmonary tuberculosis of 411 cases. Ann Clin Microbiol Antimicrob 2015;14:34.
16. Shrivastava A, Brahmachari S, Pathak P, Kumar R, Sainia T, Patel U, *et al*. A clinico-epidemiological profile of extra-pulmonary tuberculosis in central India. Int J Med Res Rev 2015;3:223-30.
17. Baykan AH, Sayiner HS, Aydin E, Koc M, Inan I, Erturk SM. Extrapulmonary tuberculosıs: An old but resurgent problem. Insights Imaging 2022;13:39.
18. Ma MJ, Xie LP, Wu SC, Tang F, Li H, Zhang ZS, *et al*. Toll-like receptors, tumor necrosis factor-α, and interleukin-10 gene polymorphisms in risk of pulmonary tuberculosis and disease severity. Hum Immunol 2010;71:1005-10.
19. Pacheco AG, Cardoso CC, Moraes MO. IFNG +874T/A, IL10 -1082G/A and TNF -308G/A polymorphisms in association with tuberculosis susceptibility: A meta-analysis study. Hum Genet 2008;123:477-84.
20. Shamseeda A, Jayasree AK. Epidemiological profile of extrapulmonary tuberculosis and its association with diabetes in tertiary care center in Northern Kerala. Int J Community Med Public Health 2022;9:2590-5.
21. Mohandas B, Pawar AT, John A, Kumar D. Treatment outcome of tuberculosis patients treated under DOTS in Calicut. Int J Community Med Public Health 2017;4:1479-9.

Access this article online

Quick Response Code:

Website: https://journals.lww.com/hrcm/

DOI: 10.4103/JHCR.JHCR_8_25

How to cite this article: Saju CR. Tuberculosis beyond lungs: An ancient but unremitting problem. J Adv Health Res Clin Med 2025;XX:XX-XX.

Review Article

Targeting the Tumor Microenvironment in Lung Cancer with a Focus on Immune Evasion, Hypoxia, and Treatment Resistance

Davis Anu[1], Kizhakkepeedika Davis Rennis[2], Valappan Veetil Soumya[1], Baby Jisna[1], K. P. Safna Hussan[1,3], Leena Chandrasekharan[1,4], Thekkekara Devassy Babu[1]

[1]Deparment of Biochemistry, Amala Cancer Research Centre, [2]Department of Pulmonology, Amala Institute of Medical Sciences, [4]Department of Veterinary Anatomy, Kerala Veterinary and Animal Sciences University, Thrissur, Kerala, India, [3]Micro/Nano Technology Center, Tokai University, Hiratsuka-shi, Japan

Abstract

As a vital organ for breathing, even brief lung failure can be fatal, highlighting the urgent need for effective lung cancer treatment. Targeting classical molecules such as epidermal growth factor receptor, anaplastic lymphoma kinase, and programmed cell death protein-1/ligand 1, as well as Kirsten rat sarcoma virus, has shown promise in treatment. However, their effectiveness is often limited by specific mutations, tumor diversity, and resistance. Recent studies highlight the tumor microenvironment (TME) as a niche of functioning cells, growth factors, and matrix that promotes cancer progression and drug resistance. In lung, the TME is especially important due to constant exposure to allergens and pathogens, which lead to an immune-rich environment and persistent inflammation. Cancer-associated fibroblasts, immune and endothelial cells, and the extracellular matrix (ECM) are the key components of TME. The TME in lung cancer is constantly changing and the components such as regulatory T-cells, tumor-associated macrophages, and myeloid-derived suppressor cells work together to weaken the immune response. This interaction not only facilitates tumor growth but also poses significant challenges for effective treatment strategies. Hypoxia in the TME also activates survival pathways such as hypoxia-inducible factor-1α, vascular endothelial growth factor, Notch, Wnt, mammalian target of rapamycin, autophagy regulators and drive epithelial-mesenchymal transition. Although many TME-targeting drugs are under development, their clinical use is still limited due to the TME's dynamic nature, metabolic shifts, and spatial variability. This review highlights the key TME factors supporting lung cancer growth and resistance, underlying mechanisms, and promising treatment strategies.

Keywords: Cancer-associated fibroblasts, extracellular matrix, lung cancer, metastasis, tumor microenvironment

Introduction

According to the WHO, lung cancer accounts for 2.09 million deaths globally, and the poor survival rate is largely due to late-stage diagnosis, metastatic potential, and frequent relapse. Diverse clinical responses due to the highly heterogeneous nature, even at primary stages, largely make lung cancer management more complex and the 5-year survival rate has continued 15% for the past three decades. Broad vascularization, dense lymphatic network, complex microenvironment, and the difficulty of achieving complete surgical resection also contributes the complexity of lung cancer.[1] Most lung cancers arise from epithelial cells, particularly those of the bronchi and bronchioles, occasionally from the supporting tissues and conventionally classified as non-small cell lung cancer (NSCLC) and small cell lung cancer (SCLC). Approximately 80% of cases are NSCLC, which includes adenocarcinoma and squamous cell carcinoma. SCLC, on the other hand, is characterized by relatively small tumors that often spread, grow more rapidly, and put major treatment challenges.[2]

While classical chemotherapeutics are still in use, the treatment of lung cancer has been largely enhanced by the advanced molecular profiling methods like next generation sequencing, which make a comprehensive analysis of genome to find key

Access this article online

Quick Response Code:

Website: https://journals.lww.com/hrcm/

DOI: 10.4103/JHCR.JHCR_2_25

Address for correspondence: Dr. Thekkekara Devassy Babu, Deparment of Biochemistry, Amala Cancer Research Centre, Amalanagar P.O., Thrissur - 680 555, Kerala, India.
E-mail: babutharakan@gmail.com

Received: 04-02-2025 **Revised:** 25-04-2025
Accepted: 02-05-2025 **Published:** ***

How to cite this article: Anu D, Rennis KD, Soumya VV, Jisna B, Hussan KP, Chandrasekharan L, *et al*. Targeting the tumor microenvironment in lung cancer with a focus on immune evasion, hypoxia, and treatment resistance. J Adv Health Res Clin Med 2025;XX:XX-XX.

driver mutations, gene rearrangements, and other genetic alterations. The key molecules include epidermal growth factor receptor (EGFR), anaplastic lymphoma kinase (ALK), reactive oxygen species proto-oncogene 1 (ROS1), B-Raf proto-oncogene, (BRAF), mesenchymal-epithelial transition factor (MET), and rearranged during transfection (RET). The development of modulators or inhibitors of these targets markedly improved progression-free survival rate and quality of life in patients and reports suggests that median survival rate exceeding 3 years have now been found in a subset of patients with metastatic phase. Among these, EGFR and Kirsten rat sarcoma virus (KRAS) mutations, ALK and ROS1 rearrangements, have shown substantial clinical benefits. Likely the overall survival rate of patients with EGFR mutations, specifically exon 19 deletions and L858R point mutations, has been shown to improve by tyrosine kinase inhibitors (TKIs) (gefitinib, erlotinib, afatinib, and the third-generation TKI osimertinib).[3] Similarly, the drugs crizotinib, ceritinib, alectinib, and lorlatinib have been reported to be effectively targeted ALK rearrangements resulting in improved clinical outcomes for NSCLC ALK-positive patients.[4] A mutation in KRAS, specifically the KRAS-G12C variant, considered as un-targetable have recently become targetable with the selective inhibitors such as sotorasib.[5] Immune checkpoint inhibitors targeting programmed cell death protein-1 (PD-1)/ligand 1 (PD-L1) and cytotoxic T-lymphocyte-associated protein 4 (CTLA-4) and antibody-drug conjugates that link monoclonal antibodies to cytotoxic agents such as trastuzumab deruxtecan, have revolutionized.[6] Currently, Food and Drug Administration-approved targeted therapies are available for oncogenic alterations in eight key genes, EGFR, ALK, ROS1, BRAF, KRAS, neurotrophic tyrosine receptor kinase (NTRK), MET, and RET, primarily used in the metastatic setting. This progress has also been achieved by precision oncology, where treatment strategies are personalized based on the unique molecular profile of patient.

However, the success of target-specific treatments in lung cancer is often restricted by various factors such as adverse toxic effects and resistance mechanisms. Resistance may be primary, arising from insufficient target or co-existing mutations, or acquired, where cancer cells adept and evolve in response to therapeutic pressure. The acquired resistance emerged by the secondary mutations in driver oncogenes, leads to on-target acquired resistance. For instance, when treated lung cancer with EGFR or ALK mutations, the cells may develop new mutations within the same gene, reducing the effectiveness of the targeted drug. In EGFR, the frequently observed secondary mutations are T790M and C797S, while in ALK is L1196M and G1202R. These alterations interfere with drug binding, thereby diminishing therapeutic efficacy and making the cancer more difficult to treat.[7] Off-target resistance also considers as challenge in treating lung cancer. A well-known example is MET proto-oncogene amplification, which is frequently observed in EGFR-mutant NSCLC in which develop resistance to TKIs. This also leads to the activation of downstream signaling pathways such as phosphoinositide 3-kinase/protein kinase b (PI3K/AKT) and mitogen-activated protein kinase. Studies suggest that MET amplification accounts for up to 20% of acquired resistance cases third-generation inhibitors like osimertinib.[8] The other contributing factors, co-dominant driver oncogenes, epithelial-mesenchymal transition (EMT), persister cancer cells, and tumor evolution underscore the complexity of resistance in targeted therapy. These limitations underscore the complexity of lung cancer biology and highlight the urgent need to explore complementary therapeutic target.

Recently, a growing body of evidence has emphasized the key role of the TME in tumor growth. TME encompasses a dynamic and multiplex network of cellular and noncellular elements such as immune and endothelial cells (EC), cancer-associated fibroblasts (CAFs,) ECM, and the molecules for signaling transduction.[9] The interactions of the structural and functional components enable the cancer cells to acquire an invasive phenotype. The regulatory T-cells (Tregs),[10] tumor-associated macrophages (TAMs), and the immune cells[11] become immunosuppressive. The TME promotes ECM remodeling, EMT, and hypoxic conditions which are closely associated with increased metastatic ability.[12] The TME also triggers signaling pathways such as nuclear factor Kappa-light-chain-enhancer of activated B-cells (NF-κB), transforming growth factor β (TGF-β), and PI3K/AKT to drive cell proliferation.[13] Recent studies on the mechanisms of interaction between cellular and noncellular components have made the TME an important hub for therapeutic interventions. This review is an attempt to examine the complex nature of the lung cancer microenvironment and elucidate its role in promoting tumor progression and therapy resistance and explore emerging therapeutic strategies.

Components of Lung Microenvironemt

Lungs maintain the physiological homeostasis by absorbing oxygen and expelling carbon dioxide within a highly sophisticated microenvironment. An array of cellular and structural components is playing key roles in maintaining the function and integrity of the lung. The important cells are alveolar epithelial cells (type I and type II), EC, immune cells (such as alveolar macrophages, dendritic cells (DCs), and lymphocytes), fibroblasts, and mesenchymal stem cells [Table 1]. Type I epithelial cells act as a thin barrier for effective gas exchange, while type II cells give wetting to decrease the surface tension. EC of pulmonary vasculature enables gas diffusion and preserving vascular architecture. Fibroblasts maintain the structural integrity of the lung by producing ECM components and serve as a barrier for toxic materials. The tissue regeneration and repair mechanisms by mesenchymal stem and other progenitor cells ensured the restoration of damaged alveolar structures.[14]

The internal environment of the lung is constantly exposed to inhaled particles such as allergens and pathogens. As a result, it is

Table 1: Components of the lung microenvironment and their function

Components	Location	Function
Epithelial cells	Alveoli (type I and II), bronchioles	Barrier function, gas exchange (type I), surfactant secretion (type II), cytokine release
ECs	Pulmonary capillaries	Form blood gas barrier, regulate vascular tone and permeability
Fibroblasts	Interstitial spaces	ECM production, structural support, fibrosis regulation
Alveolar macrophages	Alveolar lumen	Immune surveillance, phagocytosis, anti-inflammatory signaling
Interstitial macrophages	Interstitium	Immuneregulation, interaction with fibroblasts and epithelial cells
Dendritic cells	Airways and interstitium	Antigen presentation, initiation of adaptive immune responses
Neutrophils	Recruited to alveoli and airways during inflammation	Host defense, release of enzymes and ROS
T lymphocytes (T cells)	Perivascular and interstitial spaces	Immuneregulation, cytotoxicity, cytokine production
B lymphocytes (B cells)	BALT	Antibody production, antigen presentation
Mast cells	Perivascular and submucosal areas	Allergy response, release of histamines and cytokines
MSCs	Interstitium	Immunemodulation, tissue repair, support for epithelial regeneration
ECM	Interstitium, basement membranes	Structural support, cell signaling, migration scaffold
Cytokines/chemokines	Secreted by immune and structural cells	Cell communication, inflammation regulation, immune cell recruitment
SP-A, SP-D	Alveolar fluid	Reduce surface tension, antimicrobial defense
Microbiota	Airways and alveolar surfaces	Immunemodulation, colonization resistance
Nerve fibers and neuropeptides	Bronchial and vascular walls	Regulate bronchomotor tone, inflammation, and pain

ECM: Extracellular matrix, MSCs: Mesenchymal stromal cells, BALT: Bronchial-associated lymphoid tissue, ROS: Reactive oxygen species, SP: Surfactant protein, ECs: Endothelial cells

uniquely enriched with immune cells. Alveolar macrophages serve as the first line of defense by engulfing and clearing pathogens, while DCs bridge innate and adaptive immunity by capturing antigens and presenting them to T-cells. Resident memory T- and B-cells contribute to sustained immune surveillance and protection. In addition, ion channels and aquaporins in epithelial and endothelial cells help to maintain an optimal alveolar hydration. This coordinated interplay of immune and structural components becomes immunologically significant. Collectively, this intricate and dynamic network of cells and signaling molecules forms the foundation of the normal lung microenvironment, which is essential not only for respiration but also for immune homeostasis and tissue integrity under both physiological and stress conditions.[15]

Due to the constant exposure to inhaled particles such as allergens and pathogens, the internal environment of the lung is particularly rich with immune cells. By engulfing pathogens alveolar macrophages act as the first line of defense. The DCs captured the antigens and presenting them to T-cells for adaptive immune responses. The memory T- and B-cells that reside in the lungs give constant support for immune surveillance and protection. The ion channels and aquaporins in epithelial and endothelial cells maintained alveolar hydration in optimum. This coordinated function ensures immunological vigilance and the balanced environment prevents unnecessary inflammation.[16] Together, this complex and dynamic network of cells and signaling molecules forms the normal lung microenvironment, which is crucial not only for respiratory function but also for maintaining immune homeostasis and tissue integrity.

Lung Tumor Microenvironment

As lung cancer develops, the normal lung microenvironment undergoes various changes, giving rise to a complex TME. Cancer cells actively remodel their surroundings by recruiting and reprogramming immune cells, fibroblasts, and EC to create an immunosuppressive and protumorigenic niche. This adaptation is driven by hypoxia, chronic inflammation, altered metabolism, and interaction between tumor and stromal cells. Such dynamic alterations enable cancer cells not only to evade immune surveillance but also to gain invasive and metastatic capabilities. Understanding how tumor cells and their microenvironment co-evolve is critical to developing more effective therapeutic strategies aimed at disrupting these adaptive mechanisms.[9]

The cellular elements of TME include CAFs, EC, pericytes, cancer stem cells, Tregs, TAMs, myeloid-derived suppressor cells (MDSCs), DCs, and tumor-infiltrating lymphocytes (TILs), such as cytotoxic T-cells (CD8+), helper T-cells (CD4+), and natural killer cells.[11] ECM, cytokines, chemokines, growth factors, hypoxic conditions, and metabolic factors are the noncellular components. The tumor-infiltrating lymphocytes (TILs), particularly CD8+ and CD4+ T-cells, play a crucial role in shaping disease progression.[17,18] Tertiary lymphoid structures (TLS), developed in the tissues by chronic inflammation and aggregates of lymphocytes, DCs, and stromal cells, are organized into distinct zones such as B- and T-cell zones and endothelial venules [Table 2].

Cellular components

Tumor-infiltrating lymphocytes

TILs are a diverse set of immune cells, largely T-cells, that intrude the TME in response to tumor-derived antigens with an

Table 2: Key components of the tumor microenvironment and their functions in lung cancer

TME component	Location in TME	Function in lung cancer
CAFs	Tumor stroma	Promote tumor growth, drug resistance, ECM remodeling, and immune evasion by secreting TGF-β, IL-6, and VEGF
ECs	Lining tumor blood vessels	Promote tumor angiogenesis and regulate drug delivery via VEGF and notch signaling
Pericytes	Surrounding ECs in vessels	Support angiogenesis, maintain vascular integrity, and contribute to drug resistance
CSCs	Tumor niche and hypoxic zones	Drive tumor heterogeneity, therapy resistance, and metastasis via EMT and stemness-related pathways.
Fibroblasts	Tumor stroma	Modify ECM, enhance tumor stiffness, and promote resistance to chemotherapy
DCs	Lymphoid-rich regions of TME	Dysfunctional DCs fail to activate effective anti-tumor immune responses
TANs	Tumor periphery and stroma	Exhibit pro-tumor (N2) or anti-tumor (N1) roles, influence immune response and angiogenesis
ECM	Throughout tumor and stromal regions	Provides structural support, affects drug penetration, and regulates cell signaling
Hypoxic regions	Poorly vascularized areas within the tumor	Induce therapy resistance, metabolic reprogramming, and immune escape via HIF-1α signaling
Adipocytes	Peritumoral adipose tissue	Supply fatty acids for tumor metabolism and contribute to drug resistance
MSCs	Recruited from bone marrow to tumor stroma	Enhance tumor progression by differentiating into fibroblasts and secreting pro-tumorigenic factors
Cytokines and chemokines	Secreted into TME	Regulate immune cell recruitment, chronic inflammation, and resistance to immunotherapy
Growth factors (e.g., VEGF, TGF-β, EGF, FGF)	Widely distributed in TME	Drive angiogenesis, tumor cell proliferation, and EMT
Metabolic components (lactate, glucose, lipids)	Tumor core and surrounding stroma	Support metabolic adaptation, acidosis, and immune suppression

CAFs: Cancer-associated fibroblasts, CSCs: Cancer stem cells, DCs: Dendritic cells, TANs: Tumor-associated neutrophils, ECM: Extracellular matrix, MSCs: Mesenchymal stem cells, TGF-β: Transforming growth factor β, EGF: Epidermal growth factor, VEGF: Vascular EGF, IL-6: Interleukin-6, EMT: Epithelial-mesenchymal transition, TME: Tumor microenvironment, HIF-1α: Hypoxia-inducible factor-1α, FGF: Fibroblast growth factor, TME: Tumor microenvironment, ECs: Endothelial cells

antitumor immune response.[19] Among these, $CD8^+$ cytotoxic T-lymphocytes (CTLs) kill tumor cells through granzyme and are reported to be associated with improved patient outcomes. $CD4^+$ helper T-cells assist CTLs and other immune cells, while some subgroups, like Th2 or Th17 cells, may aid in tumor progression. On the contrary, Tregs, expressing CD4, CD25, and FOXP3, suppress immunity by reducing the activity of effector T-cells and adopting immune tolerance in TME. Tumor antigen exposure may lead to the failure of TILs function, which is depicted by the expression of inhibitory receptors PD-1, T-cell immunoglobulin and mucin-domain containing-3 (TIM-3), and lymphocyte-activation gene 3 (LAG-3). Hypoxia and the metabolically competitive nature of TME change TILs function. Thus, understanding the composition and functional status of TILs within the lung TME is critical for developing effective immunotherapeutic strategies.

Regulatory T-cells

Tregs are a subset of $CD4^+$ T-cells that maintain immune tolerance and prevent autoimmunity. However, in TME, particularly in NSCLC, Tregs assist immune escape and tumor progression by expressing transcription factor FoxP3, CD25 (interleukin-2 [IL-2] receptor-α), and reduced expression of CD127. Then, the tumor cells and stromal parts actively recruit Tregs by secreting chemokines while TGF-β and IL-10 promote their expansion and stabilization. Once localized, Tregs decrease responses of cytotoxic $CD8^+$ T cells and Th1 effectors. An interaction of Tregs with DCs reported impairs antigen presentation and co-stimulation, while their high expression of immune checkpoints such as CTLA-4 leads to downregulation of CD80/CD86. Various reports suggested that poor prognosis and reduced survival of patients are reported to be associated with elevated Treg infiltration. Depleting or functionally inhibiting Tregs, particularly in combination with immune checkpoint inhibitors (anti-PD-1 or anti-CTLA-4 antibodies), is under investigation.[20]

Tumor-associated macrophages

TAMs, a central component of TME, originate primarily from circulating monocytes, then are recruited to the tumor site, where they are alerted by local signals. These macrophages are polarized classically to M1-like, which are pro-inflammatory and anti-tumorigenic and produce IL-12 and TNF-α and help Th1 immune responses. Some are alternatively activated to M2-like macrophages, which are anti-inflammatory and pro-tumorigenic. They secrete IL-10, TGF-β, and other factors that suppress immune responses and support tissue remodeling, angiogenesis, and metastasis. In lung cancer, TAMs are predominantly M2-polarized, which support immunosuppressive effects, angiogenesis, the secretion of vascular endothelial growth factor (VEGF) and matrix metalloproteinases (MMPs), and ECM remodeling. M2

phenotypes reduce the activity of cytotoxic T-cells and promote the expansion of Tregs, enhance EMT by releasing factors such as TGF-β and IL-6, aid tumor cell dissemination and contribute to chemoresistance and resistance to immune checkpoint inhibitors by expressing immune checkpoints (e.g., PD-L1) or secreting survival signals.[21] Various therapeutic strategies of TAM targeting drugs are listed by Zhu *et al*.[22] Clinically high TAM infiltration, especially M2-like, correlates with poor prognosis and reduced survival in lung cancer patients. Targeting TAMs either by depleting them, reprogramming M2 to M1, or blocking their recruitment (*via* chemokine Ligand 2/chemokine Receptor 2 (CCL2/CCR2) axis or colony-stimulating factor-1R inhibitors) is emerging as a promising therapeutic approach in lung cancer.[23]

Myeloid-derived suppressor cells

MDSCs, a heterogeneous population of immature myeloid cells in lung TME, inhibit T-cell activation and proliferation, which facilitates immune evasion.[24] The main mechanism involved is the reduction of essential amino acids. MDSC express a high level of arginase 1 (Arg1), which metabolizes L-arginine, a key amino acid for T-cells. The reduction of L-arginine results in the downregulation of the T-cell receptor (TCR) ζ-chain, which impairs T-cell activation. Furthermore, MDSCs consume extracellular cystine but fail to release cysteine, depriving T-cells. Another mechanism is the production of ROS and NO, which can induce T-cell apoptosis, inhibit proliferation, and impair TCR signaling. MDSC further inhibit T-cell responses and promote the development of Tregs by secreting TGF-β and IL-10. MDSC reported to express PD-L1, which binds to PD-1 on T-cells, also leads to T-cell exhaustion. The VEGF and MMP9 produced by MDSC promote angiogenesis. The accumulation and persistent activity of MDSC are associated with poor clinical outcomes, as these cells not only dampen anti-tumor immune responses but also promote tumor angiogenesis and metastasis. Consequently, targeting MDSCs has emerged as a promising therapeutic approach to enhance the effectiveness of current cancer immunotherapies. Due to a multifaceted role, MDSCs are considered a promising target.[25]

Cancer-associated fibroblasts

CAF, a heterogeneous population of activated fibroblasts in TME that support tumor progression, especially by metabolic reprogramming and remodeling of ECM. CAF specially converts glucose to high-energy metabolites lactate and pyruvate even in the presence of oxygen. The adoption of aerobic glycolysis is commonly known as the Warburg effect. Thus, the tumor cells use anabolic processes to boost proliferation and survival. CAFs were also found to release free fatty acids and other lipid molecules which may serve as an alternative energy source for more aggressive cancer phenotypes. CAF also remodel the ECM by largely secreting collagens, fibronectin, and proteoglycans for stiffening, which enhances tumor cell invasion. For this, CAFs secrete MMPs to degrade ECM, which leads to the release of ECM-bound growth factors. This process promotes tumor progression and makes a physical barrier for the effective delivery of therapeutic agents. The metabolic reprogramming and ECM remodeling by CAFs create a TME.[26] Targeting these CAF-mediated processes offers promising avenues for developing novel therapeutic strategies aimed at disrupting the supportive role of CAFs in cancer.

Endothelial cells

EC are the inner lining of blood vessels. In lung, ECs favor neovascularization by hypoxia and pro-angiogenic factors, especially VEGF. This new vasculature supplies oxygen and nutrients for tumor growth and metastasis. By expressing adhesion molecules such as intercellular adhesion molecule-1, vascular cell adhesion molecule-1, and secreting cytokines and growth factors, EC create a pro-tumorigenic microenvironment. Recent studies suggest that EC can alter immune cell trafficking and polarization for immunosuppressive niches. To maintain this angiogenesis, EC undergo metabolic reprogramming to meet the heightened demands for energy and biomass, which poses significant challenges to successful cancer therapy.[27]

Pericytes

Pericytes are seen closely associated with EC, especially in capillaries and venules, for preserving vascular stability, integrity, and permeability. In lung cancer, aberrant coverage of pericytes is actively supporting angiogenesis, metastasis, and therapeutic resistance. Moreover, loss or dysfunction of coverage leads to tumor cell intravasation into the bloodstream. Recent studies indicate that pericyte-rich tumors may be more resistant to anti-angiogenic therapies. Pericytes also contribute to immunomodulation and immune cell trafficking by secreting cytokines such as TGF-β and IL-10.

Cancer associated adipocytes

Adipocytes, the energy-storing fat cells, which are actively participating in the TME of the lung, which secretes bioactive molecules such as adipokines (leptin and adiponectin), pro-inflammatory cytokines (IL-6, TNF-α), chemokines, and free fatty acids for tumor growth. Leptin, for instance, activates Janus kinase/signal transducer and activator of transcription (JAK/STAT) and PI3K/AKT for the proliferation and survival of cancer cells. These adipocytes alter their phenotype and enhance lipolysis, which releases free fatty acids as metabolic fuel for cancer cells *via* fatty acid oxidation. Adipocyte produced cytokines such as IL-1β and monocyte chemoattractant protein-1 (MCP-1) that supports chronic inflammation and recruit TAM and MDSCs.[28] Adipocytes also alter ECM and interact with other stromal components to promote angiogenesis and metastatic spread. Emerging evidence suggests that visceral adiposity, especially in lung adenocarcinoma, correlates with poor prognosis and altered immune cell profiles.

Noncellular components

Extracellular matrix

ECM is a complex architecture with various macromolecules such as structural proteins, adhesive glycoproteins, proteoglycans, and glycosaminoglycans. Tumor-associated

remodeling of ECM releases several growth factors, including VEGF and TGF-β, enabling angiogenesis, EMT, and metastasis and reported to trigger mechanotransduction pathways of focal adhesion kinase/Src family kinases (FAK/Src) and yes-associated protein/transcriptional co-activator with PDZ-binding motif (YAP/TAZ) promoting tumor growth. ECM interacts with integrins and cell surface receptors for intracellular signaling cascades that enhance survival and immune evasion. In lung cancer, increased deposition of collagen and fibronectin correlates with tumor aggressiveness and poor clinical outcomes. This highlighting the ECM as a crucial regulator of tumor biology and a potential therapeutic target.[29]

Cytokines and growth factors

Cytokines and growth factors are soluble mediators within the TME to organize the signal transduction process for cancer development and progression. Among them, the activation of TGF-β leads to a tumor suppressor in early stages. However, at a later stage, it is reported to act as a promoter of invasion, EMT, immune suppression, and metastasis by activating SMAD and non-SMAD signaling pathways. VEGF, produced by tumor cells and stromal constituents under hypoxic states, directs angiogenesis. Thus, targeting VEGF (bevacizumab) has shown benefits in lung cancer patients. In addition, interleukins such as IL-6, IL-1β, and IL-10 are frequently elevated in lung cancer; IL-6, in particular, activates the JAK/STAT3 pathway, leading to resistance to apoptosis.[30] IL-1β recruits MDSCs, while IL-10 inhibits anti-tumor immune responses. Together, these mediators increase tumor growth, angiogenesis, metastasis, and immune evasion, making them attractive targets for therapeutic intervention in lung cancer.

Proteases

Proteases, specifically MMPs, are zinc-dependent endopeptidases that have a key role in remodeling ECM. In the lung, MMPs are produced by tumor cells and also by various stromal components, which degrade ECM components, leading to the breakdown of physical barriers and allowing tumor cell invasion and metastasis. Among these, MMP-2 (gelatinase A) and MMP-9 (gelatinase B) specifically degrade type IV collagen, a major component of the basement membrane in the lung.[31] Overexpression of MMPs correlated with poor prognosis in NSCLC. MMPs also reported to modulate the availability of growth factors and cytokines by releasing them from the ECM. Moreover, the ECM degradation products like matrikines that exert signaling effects contribute to tumor cell survival, proliferation, and resistance to therapy. As targets, MMPs have been explored, but clinically MMP inhibitors have had limited success. However, various studies are progressing to develop more selective MMP-targeting drugs.

Tumor Microenvironment and Immune Evasion

One of the hallmarks of the TME is its ability to facilitate immune evasion, allowing tumor cells to escape immune surveillance. TME makes a tolerogenic environment to inhibits anti-tumor immune responses by the recruitment and modulation of various immunosuppressive cells such as Tregs, TAMs, and MDSCs. The understanding of these molecules and their immune evasion mechanisms is crucial for the development of target-specific effective immunotherapies in lung cancer. The important proteins and pathways involved in immune evasion are presented in Table 3.

Suppression of cytotoxic immune responses is a key strategy employed by the TME to facilitate immune evasion.[32] TAMs, predominantly of the M2 phenotype, secrete anti-inflammatory cytokines such as TGF-β and IL-10, which inhibit CTL activation. Similarly, Tregs release IL-10 and TGF-β, and suppress effector T-cell activity through CTLA-4–mediated signaling MDSCs further impair T-cell responses by producing immunosuppressive molecules like Arg1, ROS, and inducible nitric oxide synthase.[33] In addition to these cellular mechanisms, the upregulation of immune checkpoint molecules significantly contributes to CTL dysfunction. The interaction between PD-1 and PD-L1 promotes T-cell exhaustion, characterized by reduced proliferation, impaired cytokine production, and weakened cytotoxicity.[34] Moreover, hypoxic conditions within the TME exacerbate immune suppression by stabilizing hypoxia-inducible factor-1α (HIF-1α), which enhances PD-L1 expression and recruits immunosuppressive cells including TAMs, Tregs, and MDSCs.[35]

Metabolic byproducts such as adenosine and lactic acid significantly contribute to the immunosuppressive nature of the TME.[36] Adenosine, generated by ectonucleotidases CD39 and CD73 expressed on tumor and stromal cells, binds to A2A receptors on T-cells, thereby diminishing their activation. Lactic acid, by acidifying the TME, impairs CTL activity and enhances the suppressive functions of Tregs and MDSCs.[37] In addition, tumor-derived exosomes enriched with immunosuppressive molecules such as PD-L1, TGF-β, and miRNAs further inhibit immune cell responses. Neutrophil extracellular traps, composed of DNA and proteins released by neutrophils, promote immune tolerance. Tumor-associated DCs, lacking essential co-stimulatory signals, fail to effectively activate T-cells – a suppression amplified by Galectin-3's interaction with PD-1.[38] Collectively, these components of the TME create a multifaceted network of immunosuppression. Targeting these pathways individually or in combination offers promising avenues to restore anti-tumor immunity and enhance the efficacy of immunotherapy in lung cancer.

Tumor Microenvironment and Chemoresistance

Despite initial positive responses to various treatment modalities, many lung cancer patients eventually develop chemoresistance, resulting in reduced therapeutic efficacy. Recent studies have increasingly focused on uncovering the underlying mechanisms of resistance, aiming to enhance drug effectiveness and improve the clinical outcomes. To delay the onset of resistance or re-sensitize tumors, multidisciplinary strategies targeting specific resistance mechanisms have been

Table 3: Proteins and pathways involved in immune evasion in lung cancer

Proteins	Mechanism of immune evasion in lung cancer	Pathway involved
PD-L1 (CD274)	Binds to PD-1 on T-cells, inhibiting their activation and promoting immune escape	PD-1/PD-L1 checkpoint
CTLA-4	Competes with CD28 for B7 binding, reducing T-cell activation and proliferation	CTLA-4 immune checkpoint
VEGF (VEGFA)	Suppresses dendritic cell maturation, promotes Treg recruitment, and enhances angiogenesis	VEGF/VEGFR signaling
HIF1A	Induces hypoxia-mediated immune suppression by increasing PD-L1 expression and recruiting MDSCs	Hypoxia signaling
TGF-β (TGFB1)	Suppresses cytotoxic T-cells and NK cell activity, promotes Treg expansion	TGF-β/SMAD signaling
IL-6	Activates STAT3 signaling, leading to immunosuppressive TME and M2 macrophage polarization	JAK/STAT signaling
CXCL12 (SDF-1)	Recruits immunosuppressive myeloid cells (MDSCs, Tregs), promoting tumor survival	CXCR4/CXCL12 axis
MMP-9	Remodels ECM, facilitates immune evasion by creating a barrier against immune cell infiltration	ECM degradation
CD44	Maintains cancer stemness, facilitates immune escape through EMT and resistance to apoptosis	EMT/cancer stem cell pathway
YAP1	Suppresses antigen presentation, promotes immune-resistant tumor growth	Hippo/YAP signaling
FOXM1	Enhances DNA repair and cell cycle progression, making cancer cells resistant to immune attack	PI3K/AKT, MAPK signaling
MYC	Downregulates MHC-I expression, reducing tumor antigen presentation	Oncogenic signaling
FAP	Supports CAF-mediated immune suppression and ECM remodeling	CAF-mediated signaling
CD73 (NT5E)	Converts ATP to immunosuppressive adenosine, reducing T-cell activity	Purinergic signaling
CSF1R	Induces TAM polarization toward an immunosuppressive (M2) phenotype	TAM-mediated immune evasion
Galectin-3 (LGALS3)	Promotes T-cell exhaustion and immune escape via TIM-3 and LAG-3 interactions	Galectin signaling
IDO1	Metabolizes tryptophan into kynurenine, suppressing T-cell proliferation	Tryptophan metabolism
LAG-3	Inhibits T-cell activation by binding to MHC-II molecules	Immune checkpoint
TIM-3 (HAVCR2)	Induces T-cell exhaustion when binding to Galectin-9	Immune checkpoint

PD-1: Programmed cell death protein-1, VEGF: Vascular epidermal growth factor, HIF-1α: Hypoxia-inducible factor-1α, IL-6: Interleukin-6, MMP-9: Matrix metalloproteinase 9, TME: Tumor microenvironment, ECM: Extracellular matrix, FAP: Fibroblast activation protein, EMT: Epithelial-mesenchymal transition, CAF: Cancer-associated fibroblast, CSF: Colony-stimulating factor, LAG-3: Lymphocyte Activation Gene 3, MDSCs: Myeloid-derived suppressor cells, AKT: Protein kinase b, MAPK: Mitogen-activated protein kinase, TGF-β: Transforming growth factor β, CTLA: Cytotoxic T-lymphocyte–associated protein 4, VEGFR: Vascular endothelial growth factor receptor, YAP: Yes-associated protein, JAK: Janus kinase, STAT: Signal transducer and activator of transcription

employed.[39] The key contributors to therapy resistance include alterations in the TME, high mutational burden, defective DNA mismatch repair, and epigenetic reprogramming. Critical signaling pathways such as PI3K-Akt, interferon, and Wnt/β-catenin have been implicated in resistance development. Additional factors such as reduced antigen presentation, upregulation of PD-L1, and epigenetic and immune checkpoint alterations further contribute to therapeutic failure [Table 3].[40] Various immunosuppressive cells within the TME – including TAMs, Tregs, regulatory B-cells, CAFs, and MDSCs – play a central role in promoting resistance. These cells inhibit effector T cell function and secrete immunosuppressive molecules such as TGF-β, IL-10, prostaglandin E2, and VEGF, thereby impairing anti-tumor immunity. Moreover, they enhance the expression of immune checkpoint proteins such as LAG-3, CTLA-4, PD-1, PD-L1, and TIM-3, further shifting the TME from an immunosupportive to an immunosuppressive state.[41]

Hypoxic zones within the TME play a pivotal role in promoting chemoresistance in lung cancer.[42] HIF-1α, a key regulator under low oxygen conditions, has been shown to upregulate drug resistance genes such as P-glycoprotein and ATP-binding cassette transporters, which actively mediate drug efflux from the cancer cells. In conjunction with TGF-β, hypoxia also induces EMT, pushing cancer cells toward a more mesenchymal and drug-resistant phenotype. Furthermore, the irregular vasculature within hypoxic regions activates adaptive survival mechanisms, contributing to reduced drug delivery and increased genetic instability. These changes collectively enhance the tumour's resistance to chemotherapy. Under hypoxic conditions, transcription factors such as HIF-1α become stabilized, promoting metabolic reprogramming toward glycolysis and upregulating survival-promoting molecules such as glucose transporter-1, VEGF, and carbonic anhydrase IX .[43]

In response to hypoxia and microenvironmental stress, the NF-κB pathway becomes activated, enhancing the expression of anti-apoptotic genes and pro-inflammatory cytokines. This activation fosters tumor cell survival and sustains a pro-inflammatory milieu that contributes to chemoresistance in lung cancer.[44] Additionally, hypoxic conditions stimulate the PI3K/AKT pathway, which facilitates cellular adaptation by promoting proliferation, metabolic rewiring, and resistance to therapy. This pathway frequently intersects with other survival networks, such as the mammalian target of rapamycin, to help tumor cells endure chemotherapy-induced stress.[45] These interrelated unusual mechanisms collectively contribute to a strong chemo-resistant phenotype in lung cancer. Therapeutic approaches targeting hypoxia-related pathways, such as inhibitors of HIF-1α, VEGF, TGF-β, NF-κB, or PI3K/AKT signaling, are being investigated to counteract chemoresistance and improve outcomes for lung cancer patients.[46] Moreover, the TGF-β/ suppressor of mothers against decapentaplegic (SMAD) and Wnt/β-catenin signaling pathways, in cooperation

with transcription factors such as zinc finger E-box-binding homeobox 1 (ZEB1) and snail family transcriptional repressor 1 (SNAIL), have been shown to suppress pro-apoptotic genes and reprogram cellular metabolism within the TME. These changes contribute to acidosis, further reinforcing resistance mechanisms and diminishing drug effectiveness.[47] Adding to this complexity, tumor-derived exosomes enriched with microRNAs – such as miR-21 – can transfer resistance traits to neighboring cells by activating survival pathways such as PI3K/AKT, thereby expanding the chemo-resistant phenotype across the tumor mass[48] [Figure 1].

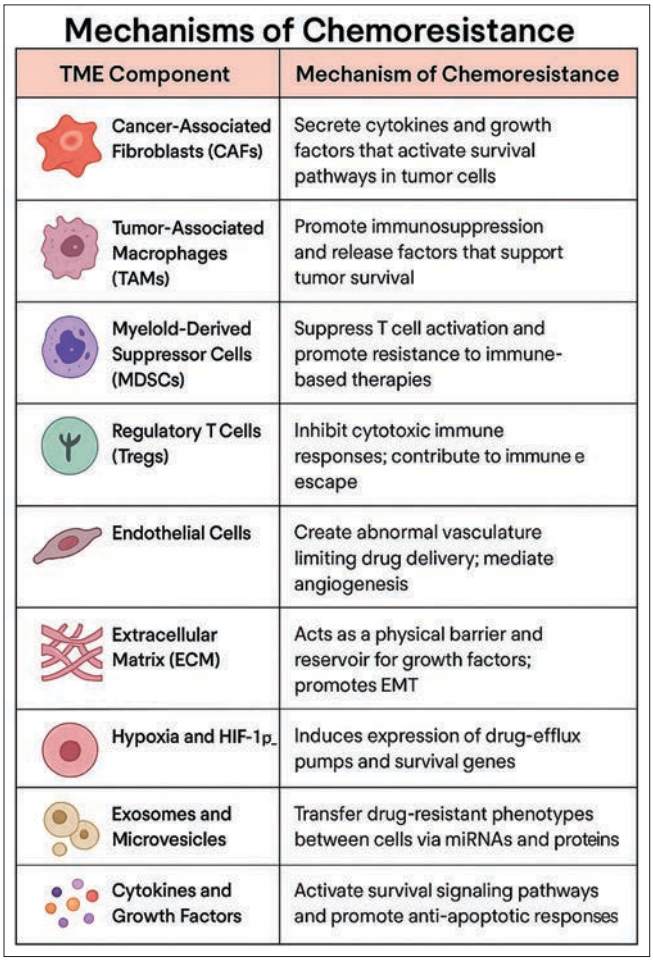

Figure 1: Mechanisms of chemoresistance mediated by tumour microenvironment (TME) components. Illustrates the key components of the TME and their respective roles in promoting chemoresistance. Cancer-associated fibroblasts, Tumour-associated macrophages, Myeloid-derived suppressor cells, regulatory T cells, endothelial cells, extracellular matrix, hypoxia-induced factors, exosomes/micro-vesicles, and various cytokines/growth factors contribute to resistance through distinct but often overlapping mechanisms. These include activation of survival pathways, suppression of cytotoxic immune responses, physical barriers to drug delivery, metabolic reprogramming, and intercellular transfer of resistance traits. Key mediators and signaling pathways involved in each component's role are indicated. HIF: Hypoxia-inducible factor, EMT: Epithelial-mesenchymal transition

Tumor Microenvironment and Metastasis

EMT plays a pivotal role in numerous physiological and pathological processes, including embryonic development, tissue and organ formation, neural crest migration, tissue remodeling, and organ fibrosis. In cancer, EMT is closely associated with metastasis and the acquisition of stem cell-like properties. During this transition, epithelial cells lose their characteristic cell-cell adhesion and polarity, accompanied by a shift in gene expression profiles. Notably, epithelial markers such as E-cadherin are downregulated, while mesenchymal markers including N-cadherin, vimentin, and fibronectin are upregulated.[49] Various studies examined the signaling pathways and associated factors that are involved in lung cancer EMT [Table 2]. In lung cancer, EMT is orchestrated by a network of signaling pathways and transcriptional regulators. Key transcription factors such as Snail, TWIST, and ZEB are activated, driving the phenotypic switch essential for tumor progression and dissemination.[50]

TME plays a central role in initiating and sustaining EMT, a process that endows tumor cells with mesenchymal characteristics such as enhanced motility, invasiveness, and resistance to therapy, while diminishing epithelial traits like adhesion and polarity. Key mediators released by CAFs, including TGF-β, hepatocyte growth factor, and fibroblast growth factor, activate signaling cascades that drive EMT.[51] Among these, TGF-β is particularly crucial, as it induces EMT-associated transcription factors such as Snail, Slug, and Twist, and modulates the expression of epithelial and mesenchymal markers including E-cadherin and vimentin.[52] In addition, immune cells within the TME – such as TAMs, MDSCs, and Tregs further support EMT through the secretion of cytokines like IL-6 and TGF-β.[53]

Hypoxia within the TME exacerbates EMT by stabilizing HIF-1α, which interacts with EMT-associated transcription factors to drive the transition.[54] MMPs further support this process by degrading extracellular matrix (ECM) components and releasing pro-EMT factors like TGF-β. Key signaling pathways, including TGF-β, NF-κB, and PI3K/AKT, play a central role in regulating EMT by altering the gene expression profiles and cytoskeletal architecture, thereby enhancing the invasive and metastatic potential of tumor cells. Targeting these TME-mediated signaling networks offers a promising strategy to suppress EMT, curb lung cancer progression, and improve therapeutic efficacy.[55] Among these, TGF-β, NF-κB, and PI3K/AKT stand out as the pivotal drivers of EMT and tumor invasion, positioning them as critical targets for intervention[56] [Figure 2].

Therapeutic Strategies Targeting Tumor Microenvironment

Recent studies have largely engaged in targeting the TME for lung cancer treatment. Disturbing the TME ecosystem is considered a promising strategy. The notable approach is restoring the anti-tumor activity of the immune cells Tregs, TAMs, and

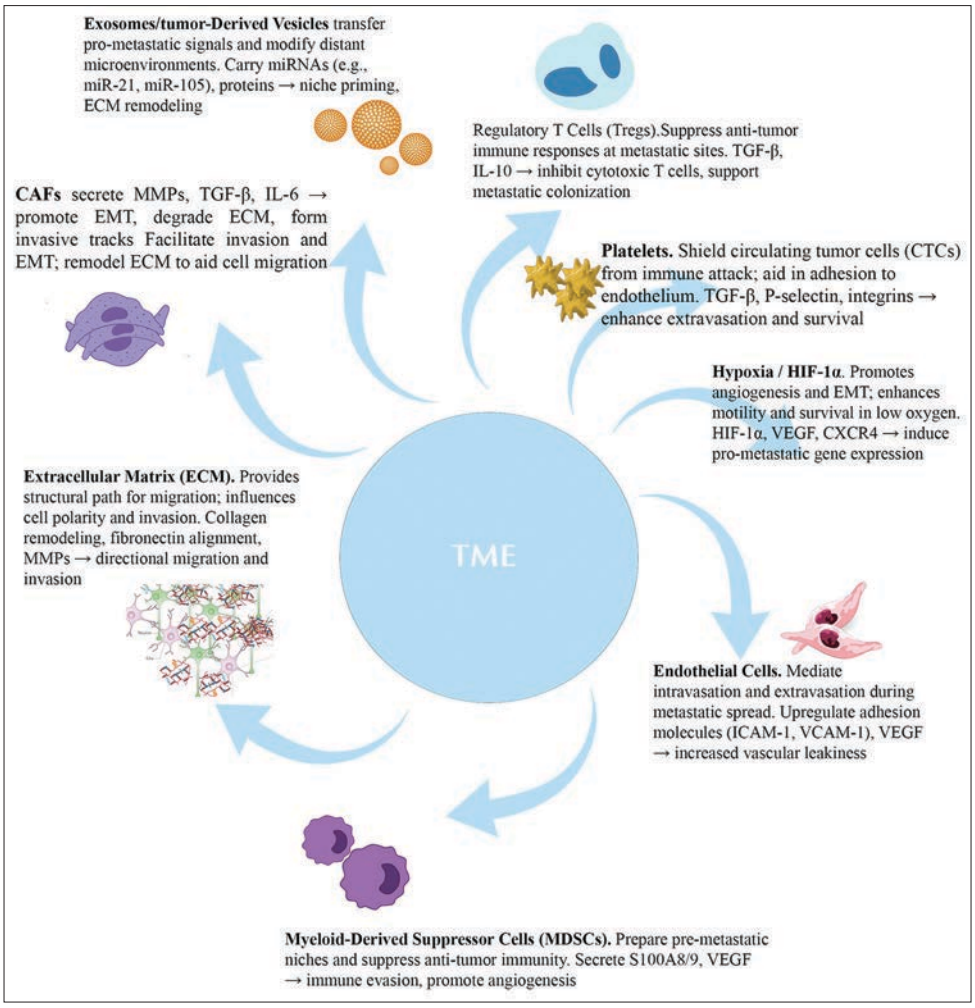

Figure 2: Key components of the tumour microenvironment (TME) in promoting metastasis and their mechanisms of action in lung cancer. This figure illustrates the critical roles of TME components in lung cancer metastasis. Cancer-associated fibroblasts remodel extracellular matrix and promote epithelial-mesenchymal transition via matrix metalloproteinases and transforming growth factor β (TGF-β). Tumour-associated macrophages enhance invasion and premetastatic niche formation through vascular endothelial growth factor (VEGF) and epidermal growth factor (EGF). Endothelial cells support intravasation via Intercellular Adhesion Molecule-1 and VEGF. Myeloid-derived suppressor cells and regulatory T cells enable immune evasion through VEGF, interleukin 10, and TGF-β. Hypoxia activates hypoxia-inducible factor-1α, driving angiogenesis and migration. Exosomes deliver pro-metastatic signals (e.g., miR-21), while platelets shield circulating tumor cells (CTCs) and aid extravasation. These elements synergize to support tumor dissemination and colonization. VEGF: Vascular endothelial growth factor, EMT: Epithelial-mesenchymal transition, HIF: Hypoxia-inducible factor, TGF-β: Transforming growth factor β, IL-10: Interleukin 10, MMPs: Matrix metalloproteinases

MDSCs by reprogramming. For instance, reverting the M2 of TAMs to M1 phenotype and developing inhibitors for immune checkpoints such as anti-PD-1, anti-PD-L1, and anti-CTLA-4 antibodies shows more promise.[23] The bispecific antibodies such as AK104 targeting PD-1 and CTLA-4 and GEN1046 targeting PD-L1 and 4-1BB are under clinical investigation. Restoring the disorganized, leaky, and hypoxic vasculature to normal architecture reported improved oxygenation, drug delivery, and immune cell infiltration. Anti-VEGF agents like bevacizumab are in clinical use. Targeting key signaling pathways has also shown therapeutic promise. TGF-β inhibitors found to prevent EMT and improve the sensitivity of the cancer cells to cell death and inhibition of NF-κB is reported to control pro-inflammatory signals. Similarly, inhibiting the PI3K/AKT pathway reduces chemoresistance and tumor adaptability.[57]

Chimeric antigen receptor T (CAR-T) cell therapy is being dynamically improved by the development of new CAR designs and combinations.[58] However, their success in solid tumors like lung cancer is restrained due to poor T-cell infiltration into the tumor site and the immunosuppressive nature of the TME. To tackle these issues, investigators are aiming to develop next-generation CAR-T cells, including dual-targeting, armored CAR-T cells and switchable or inducible CARs that allow external control over CAR-T cell activation. However, linking CAR-T therapy with other strategies like immune checkpoint inhibitors, VEGF blockers, or agents that modulate the TME is being explored to enhance CAR-T cell persistence, trafficking, and tumor-killing ability. These innovations suggest that CAR-T cell therapy is more effective for solid tumors, like lung cancer. These

Table 4: Therapeutic strategies targeting tumor microenvironment

TME component	Therapeutic strategy	Target(s)	Examples of agents/approaches
CAFs	Inhibition of CAF activation and signaling	TGF-β, FAP, PDGFR	Galunisertib (TGF-β inhibitor), FAP-targeted CAR-T cells
TAMs	Reprogramming or depletion of TAMs	CSF-1R, CD47, TLRs	Pexidartinib (CSF-1R inhibitor), anti-CD47 antibodies
MDSCs	Inhibition of recruitment/function	Arginase-1, STAT3, CXCR2	Arginase inhibitors, STAT3 inhibitors, SX-682 (CXCR1/2)
Regulatory T cells (Tregs)	Suppression or depletion	CTLA-4, CD25	Ipilimumab (anti-CTLA-4), anti-CD25 antibodies
EC	Vascular normalization	VEGF, Angiopoietins	Bevacizumab (anti-VEGF), trebananib (Ang1/2 inhibitor)
ECM	ECM remodeling or degradation	MMPs, LOX, hyaluronan	PEGPH 20 (hyaluronidase), MMP inhibitors
Hypoxia and HIF-1α	Targeting hypoxia pathways	HIF-1α, CAIX, VEGF	PX-478 (HIF-1α inhibitor), CAIX inhibitors
Exosomes and microvesicles	Inhibition of exosome biogenesis or uptake	nSMase2, Rab27a	GW4869 (exosome inhibitor), exosome-blocking antibodies
Cytokines and growth factors	Neutralization of pro-tumor cytokines/growth factors	IL-6, IL-8, TGF-β, EGF	Tocilizumab (IL-6R inhibitor), EGFR inhibitors

ECM: Extracellular matrix, MDSCs: Myeloid-derived suppressor cells, CAFs: Cancer-associated fibroblasts, TAMs: Tumor-associated macrophages, TME: Tumour microenvironment, TGF-β: Transforming growth factor β, FAP: Fibroblast activation protein, CSF: Colony-stimulating factor, IL-6: Interleukin-6, EGF: Epidermal growth factor, VEGF: Vascular EGF, CAIX: Carbonic anhydrase IX, HIF-1α: Hypoxia-inducible factor-1α, MMP: Matrix metalloproteinase, CAR-T: Chimeric antigen receptor T, EGFR: EGF receptor, ECs: Endothelial cells, TLRs: toll-like receptors

TME-targeting drugs exhibit a significant breakthrough in lung cancer management[59] [Table 4]. This strategy believes in substantial promise to improve therapeutic outcomes and achieve durable responses in lung cancer patients.

Challenges and Future Perspectives

Targeting the TME in lung cancer offers a promising strategy to disrupt tumor progression, overcome therapeutic resistance, and improve treatment outcomes. TME-targeted interventions can enhance drug delivery, modulate immune responses, and block pro-survival pathways that sustain tumor growth and metastasis. When combined with conventional therapies, these approaches hold the potential to significantly improve patient survival and quality of life. However, the heterogeneity of the TME, including its diverse cellular composition, variable signaling networks, and metabolic shifts, poses a major challenge, often limiting therapeutic efficacy. Furthermore, the adaptability of TME components may allow tumors to bypass targeted therapies through alternative pathways, necessitating combination treatments that address the multiple aspects of the microenvironment simultaneously. Advancements in molecular profiling, multi-omics technologies, and imaging are deepening our understanding of TME dynamics, enabling more precise and personalized therapeutic strategies. Current clinical trials are exploring combinations of TME-targeted agents with immunotherapies and conventional treatments to achieve synergistic effects. CAR-T-cell therapy also shows promise by enhancing tumor targeting and reshaping the immunosuppressive TME.

In conclusion, reprogramming immune responses, normalizing vasculature, and inhibiting key TME-associated pathways, particularly when combined with established therapies, offers a powerful approach for managing lung cancer. TME-targeted strategies not only reduce resistance but also improve overall treatment efficacy. Continued research into TME biology is critical to refining these approaches, paving the way for innovative and personalized lung cancer treatments.

Financial support and sponsorship

Nil.

Conflicts of interest

There are no conflicts of interest.

References

1. Reed HO, Wang L, Sonett J, Chen M, Yang J, Li L, *et al*. Lymphatic impairment leads to pulmonary tertiary lymphoid organ formation and alveolar damage. J Clin Invest 2019;129:2514-26.
2. Beadsmoore CJ, Screaton NJ. Classification, staging and prognosis of lung cancer. Eur J Radiol 2003;45:8-17.
3. Gijtenbeek RG, Damhuis RA, van der Wekken AJ, Hendriks LE, Groen HJ, van Geffen WH. Overall survival in advanced epidermal growth factor receptor mutated non-small cell lung cancer using different tyrosine kinase inhibitors in The Netherlands: A retrospective, nationwide registry study. Lancet Reg Health Eur 2023;27:100592.
4. Attili I, Fuorivia V, Spitaleri G, Corvaja C, Trillo Aliaga P, Del Signore E, *et al*. Alectinib versus lorlatinib in the front-line setting for ALK-rearranged Non-Small-Cell Lung Cancer (NSCLC): A deep dive into the main differences across ALEX and CROWN phase 3 trials. Cancers 2024;16:2457.
5. Santarpia M, Ciappina G, Spagnolo CC, Squeri A, Passalacqua MI, Aguilar A, *et al*. Targeted therapies for KRAS-mutant non-small cell lung cancer: From preclinical studies to clinical development-a narrative review. Transl Lung Cancer Res 2023;12:346-68.
6. Drago JZ, Modi S, Chandarlapaty S. Unlocking the potential of antibody-drug conjugates for cancer therapy. Nat Rev Clin Oncol 2021;18:327-44.
7. Lovly CM, Iyengar P, Gainor JF. Managing resistance to EFGR- and ALK-targeted therapies. Am Soc Clin Oncol Educ Book 2017;37:607-18.
8. Qin K, Hong L, Zhang J, Le X. MET amplification as a resistance driver to TKI therapies in lung cancer: Clinical challenges and opportunities.

Cancers (Basel) 2023;15:612.
9. Altorki NK, Markowitz GJ, Gao D, Port JL, Saxena A, Stiles B, *et al*. The lung microenvironment: An important regulator of tumour growth and metastasis. Nat Rev Cancer 2019;19:9-31.
10. Liang J, Bi G, Shan G, Jin X, Bian Y, Wang Q. Tumor-associated regulatory T cells in non-small-cell lung cancer: Current advances and future perspectives. J Immunol Res 2022;2022:4355386.
11. Zhou Y, Qian M, Li J, Ruan L, Wang Y, Cai C, *et al*. The role of tumor-associated macrophages in lung cancer: From mechanism to small molecule therapy. Biomed Pharmacother 2024;170:116014.
12. Parker AL, Cox TR. The role of the ECM in lung cancer dormancy and outgrowth. Front Oncol 2020;10:1766.
13. Sanaei MJ, Razi S, Pourbagheri-Sigaroodi A, Bashash D. The PI3K/Akt/mTOR pathway in lung cancer; oncogenic alterations, therapeutic opportunities, challenges, and a glance at the application of nanoparticles. Transl Oncol 2022;18:101364.
14. Lloyd CM, Marsland BJ. Lung homeostasis: Influence of age, microbes, and the immune system. Immunity 2017;46:549-61.
15. Gopallawa I, Dehinwal R, Bhatia V, Gujar V, Chirmule N. A four-part guide to lung immunology: Invasion, inflammation, immunity, and intervention. Front Immunol 2023;14:1119564.
16. Ardain A, Marakalala MJ, Leslie A. Tissue-resident innate immunity in the lung. Immunology 2020;159:245-56.
17. Stankovic B, Bjørhovde HA, Skarshaug R, Aamodt H, Frafjord A, Müller E, *et al*. Immune cell composition in human non-small cell lung cancer. Front Immunol 2018;9:3101.
18. Prado-Garcia H, Romero-Garcia S, Aguilar-Cazares D, Meneses-Flores M, Lopez-Gonzalez JS. Tumor-induced CD8+ T-cell dysfunction in lung cancer patients. Clin Dev Immunol 2012;2012:741741.
19. Frankowska K, Zarobkiewicz M, Dąbrowska I, Bojarska-Junak A. Tumor infiltrating lymphocytes and radiological picture of the tumor. Med Oncol 2023;40:176.
20. Li Y, Zhang C, Jiang A, Lin A, Liu Z, Cheng X, *et al*. Potential anti-tumor effects of regulatory T cells in the tumor microenvironment: A review. J Transl Med 2024;22:293.
21. Huang Z, Xiao Z, Yu L, Liu J, Yang Y, Ouyang W. Tumor-associated macrophages in non-small-cell lung cancer: From treatment resistance mechanisms to therapeutic targets. Crit Rev Oncol Hematol 2024;196:104284.
22. Zhu R, Huang J, Qian F. The role of tumor-associated macrophages in lung cancer. Front Immunol 2025;16:1556209.
23. Adams CJ, Kopp MC, Larburu N, Nowak PR, Ali MM. Structure and molecular mechanism of ER stress signaling by the unfolded protein response signal activator IRE1. Front Mol Biosci 2019;6:11.
24. Tumino N, Fiore PF, Pelosi A, Moretta L, Vacca P. Myeloid derived suppressor cells in tumor microenvironment: Interaction with innate lymphoid cells. Semin Immunol 2022;61-4:101668.
25. He S, Zheng L, Qi C. Myeloid-derived suppressor cells (MDSCs) in the tumor microenvironment and their targeting in cancer therapy. Mol Cancer 2025;24:5.
26. Mathieson L, Koppensteiner L, Dorward DA, O'Connor RA, Akram AR. Cancer-associated fibroblasts expressing fibroblast activation protein and podoplanin in non-small cell lung cancer predict poor clinical outcome. Br J Cancer 2024;130:1758-69.
27. Daum S, Decristoforo L, Mousa M, Salcher S, Plattner C, Hosseinkhani B, *et al*. Unveiling the immunomodulatory dance: Endothelial cells' function and their role in non-small cell lung cancer. Mol Cancer 2025;24:21.
28. Zhou C, He X, Tong C, Li H, Xie C, Wu Y, *et al*. Cancer-associated adipocytes promote the invasion and metastasis in breast cancer through LIF/CXCLs positive feedback loop. Int J Biol Sci 2022;18:1363-80.
29. Tanino Y. Roles of extracellular matrix in lung diseases. Fukushima J Med Sci 2024;70:1-9.
30. Bezel P, Valaperti A, Steiner U, Scholtze D, Wieser S, Vonow-Eisenring M, *et al*. Evaluation of cytokines in the tumor microenvironment of lung cancer using bronchoalveolar lavage fluid analysis. Cancer Immunol Immunother 2021;70:1867-76.
31. Nikolov A, Popovski N. Role of gelatinases MMP-2 and MMP-9 in healthy and complicated pregnancy and their future potential as preeclampsia biomarkers. Diagnostics (Basel) 2021;11:480.
32. Zhang H, Li S, Wang D, Liu S, Xiao T, Gu W, *et al*. Metabolic reprogramming and immune evasion: The interplay in the tumor microenvironment. Biomark Res 2024;12:96.
33. Malfitano AM, Pisanti S, Napolitano F, Di Somma S, Martinelli R, Portella G. Tumor-associated macrophage status in cancer treatment. Cancers (Basel) 2020;12:1987.
34. Genova C, Dellepiane C, Carrega P, Sommariva S, Ferlazzo G, Pronzato P, *et al*. Therapeutic implications of tumor microenvironment in lung cancer: Focus on immune checkpoint blockade. Front Immunol 2021;12:799455.
35. Sezer A, Kilickap S, Gümüş M, Bondarenko I, Özgüroğlu M, Gogishvili M, *et al*. Cemiplimab monotherapy for first-line treatment of advanced non-small-cell lung cancer with PD-L1 of at least 50%: A multicentre, open-label, global, phase 3, randomised, controlled trial. Lancet 2021;397:592-604.
36. Vlachostergios PJ, Oikonomou KG, Gibilaro E, Apergis G. Elevated lactic acid is a negative prognostic factor in metastatic lung cancer. Cancer Biomark 2015;15:725-34.
37. Verma NK, Wong BH, Poh ZS, Udayakumar A, Verma R, Goh RK, *et al*. Obstacles for T-lymphocytes in the tumour microenvironment: Therapeutic challenges, advances and opportunities beyond immune checkpoint. EBioMedicine 2022;83:104216.
38. Anichini A, Perotti VE, Sgambelluri F, Mortarini R. Immune escape mechanisms in non small cell lung cancer. Cancers (Basel) 2020;12:3605.
39. Mestrallet G, Brown M, Bozkus CC, Bhardwaj N. Immune escape and resistance to immunotherapy in mismatch repair deficient tumors. Front Immunol 2023;14:1210164.
40. Konen JM, Wu H, Gibbons DL. Immune checkpoint blockade resistance in lung cancer: Emerging mechanisms and therapeutic opportunities. Trends Pharmacol Sci 2024;45:520-36.
41. Tang S, Qin C, Hu H, Liu T, He Y, Guo H, *et al*. Immune checkpoint inhibitors in non-small cell lung cancer: Progress, challenges, and prospects. Cells 2022;11:320.
42. Ziółkowska-Suchanek I. Mimicking tumor hypoxia in non-small cell lung cancer employing three-dimensional *in vitro* models. Cells 2021;10:141.
43. Tirpe AA, Gulei D, Ciortea SM, Crivii C, Berindan-Neagoe I. Hypoxia: Overview on hypoxia-mediated mechanisms with a focus on the role of HIF genes. Int J Mol Sci 2019;20:6140.
44. Zhang L, Ludden CM, Cullen AJ, Tew KD, Branco de Barros AL, Townsend DM. Nuclear factor kappa B expression in non-small cell lung cancer. Biomed Pharmacother 2023;167:115459.
45. Deng H, Chen Y, Li P, Hang Q, Zhang P, Jin Y, *et al*. PI3K/AKT/mTOR pathway, hypoxia, and glucose metabolism: Potential targets to overcome radioresistance in small cell lung cancer. Cancer Pathog Ther 2023;1:56-66.
46. Bui BP, Nguyen PL, Lee K, Cho J. Hypoxia-inducible factor-1: A novel therapeutic target for the management of cancer, drug resistance, and cancer-related pain. Cancers (Basel) 2022;14:6054.
47. Shi X, Yang J, Deng S, Xu H, Wu D, Zeng Q, *et al*. TGF-β signaling in the tumor metabolic microenvironment and targeted therapies. J Hematol Oncol 2022;15:135.
48. Wang Y, Zhang T, He X. Advances in the role of microRNAs associated with the PI3K/AKT signaling pathway in lung cancer. Front Oncol 2023;13:1279822.
49. Lim SC, Jang IG, Kim YC, Park KO. The role of E-cadherin expression in non-small cell lung cancer. J Korean Med Sci 2000;15:501-6.
50. Nam MW, Kim CW, Choi KC. Epithelial-mesenchymal transition-inducing factors involved in the progression of lung cancers. Biomol Ther (Seoul) 2022;30:213-20.
51. Bordignon P, Bottoni G, Xu X, Popescu AS, Truan Z, Guenova E, *et al*. Dualism of FGF and TGF-β signaling in heterogeneous cancer-associated fibroblast activation with ETV1 as a critical determinant. Cell Rep 2019;28:2358-72.e6.
52. Naber HP, Drabsch Y, Snaar-Jagalska BE, ten Dijke P, van Laar T. Snail and slug, key regulators of TGF-β-induced EMT, are sufficient for the induction of single-cell invasion. Biochem Biophys Res Commun 2013;435:58-63.

53. He ZN, Zhang CY, Zhao YW, He SL, Li Y, Shi BL, *et al*. Regulation of T cells by myeloid-derived suppressor cells: Emerging immunosuppressor in lung cancer. Discov Oncol 2023;14:185.
54. Tam SY, Wu VW, Law HK. Hypoxia-induced epithelial-mesenchymal transition in cancers: HIF-1α and beyond. Front Oncol 2020;10:486.
55. Li F, Song QZ, Zhang YF, Wang XR, Cao LM, Li N, *et al*. Identifying the EMT-related signature to stratify prognosis and evaluate the tumor microenvironment in lung adenocarcinoma. Front Genet 2022;13:1008416.
56. Moghbeli M. PI3K/AKT pathway as a pivotal regulator of epithelial-mesenchymal transition in lung tumor cells. Cancer Cell Int 2024;24:165.
57. Ghorbaninejad M, Abdollahpour-Alitappeh M, Shahrokh S, Fayazzadeh S, Asadzadeh-Aghdaei H, Meyfour A. TGF-β receptor I inhibitor may restrict the induction of EMT in inflamed intestinal epithelial cells. Exp Biol Med (Maywood) 2023;248:665-76.
58. Zhong S, Cui Y, Liu Q, Chen S. CAR-T cell therapy for lung cancer: A promising but challenging future. J Thorac Dis 2020;12:4516-21.
59. Ma HY, Das J, Prendergast C, De Jong D, Braumuller B, Paily J, *et al*. Advances in CAR T cell therapy for non-small cell lung cancer. Curr Issues Mol Biol 2023;45:9019-38.

Original Article

Elder Abuse Screening in Domestic Settings of Kerala: Development of a New Tool

Deepa Nesan, Thomas Iype, Rema Devi Sivaraman
Department of Medical Education, Government Medical College, Thiruvananthapuram, Kerala, India

Abstract

Background: Elder abuse is a significant and pervasive issue affecting older adults' physical and psychological health in all cultures. Underreporting and underdetection are the two main challenges preventing abuse reporting, likely due to the lack of culturally appropriate screening instruments. Based on these contemplations, the present study aimed to develop and validate a culturally relevant scale for measuring elder abuse in domestic settings. **Materials and Methods:** We followed three steps for the scale development process: (a) item generation, (b) theoretical analysis, and (c) psychometric analysis. We used a sequential exploratory design with qualitative content analysis for item generation and a descriptive cross-sectional design for testing the psychometric properties of the newly developed tool. The sampling method was purposive for qualitative data collection like focus group discussion and in-depth interviews; stratified multistage sampling was used for the psychometric testing. We did an exploratory factor analysis. **Results:** Among 344 participants, 54% were females. The mean age of participants was 69.6 (standard deviation = 6.3) years. The newly developed Elder Mistreatment Screening Tool (EMST) consists of 15 items with a three-point scale. Four components explained a total variance of 72.4%. Test–retest (0.94), inter-rater reliability (0.94), and Cronbach's alpha 0.92 ensured good reliability. **Conclusion:** EMST is a psychometrically robust, culture-appropriate tool to measure elder abuse in domestic settings.

Keywords: Domestic settings, elder abuse, factor analysis, psychometrics, screening

Introduction

Kerala, a southern state of India, has the highest proportion of older adults in its population, i.e., 12.6%.[1] This aging scenario has created pressure on different aspects of care for older persons in terms of finances, health, and shelter (households are getting congested). Conventionally, Indian culture provides a sound support system for the elderly. However, accelerated migration, modernization in families, eroded traditional values, degeneration of the joint family system, and increased participation of women in economic activities make the older people a burden to the younger generation. Elder abuse is a mounting and alarming public health issue with devastating consequences for the victims and society, including increased risk of morbidity, mortality, institutionalization, loss of productivity, isolation, and despair.[2-4]

Studies indicate that elder abuse exists in the family context.[5-7] In Kerala, verbal abuse and neglect were the most common abuse, followed by physical abuse and material exploitation.[8] The primary challenge is the under-reporting of elder abuse.[9] We see only the tip of the iceberg, with only one in 24 reported elder abuse cases.[10]

Elder abuse is a multifaceted construct having a social dimension; tools developed for a population may not be valid in other cultures. Symbolic interactionism theory explains the role of culture and beliefs in the perception of abuse.[11] For example, in some cultures, sending older individuals to care homes is considered a form of abuse, whereas other cultures describe it as a symbol of caring. Mere translation of a tool developed for a population may wrongly assess elder abuse in a different culture. Most of the existing elder abuse instruments were primarily from occidental culture. The literature review discloses that the lack of a well-validated and

Address for correspondence: Dr. Deepa Nesan, Government Medical College, Thiruvananthapuram, Kerala, India.
E-mail: deepanesan@gmail.com

Received: 10-10-2024 **Revised:** 03-02-2025
Accepted: 01-03-2025 **Published:** ***

Access this article online

Quick Response Code:

Website: https://journals.lww.com/hrcm/

DOI: 10.4103/JHCR.JHCR_23_24

How to cite this article: Nesan D, Iype T, Sivaraman RD. Elder abuse screening in domestic settings of Kerala: Development of a new tool. J Adv Health Res Clin Med 2025;XX:XX-XX.

reliable scale has impeded elder abuse screening. To our best knowledge, a valid and reliable instrument on elder abuse for the Malayalam-speaking population does not exist.

Hence, we aimed to develop and validate a new scale for assessing elder abuse in a family setting in the cultural context of Kerala. The newly designed instrument should be brief and satisfy all essential psychometric properties using elder-centered approaches.

Materials and Methods

We used a mixed method approach with sequential exploratory design; beginning with qualitative methods (Phase 1)—namely focus group discussions (FGDs) and in-depth interviews (IDIs) with key stakeholders—for item generation, followed by a quantitative approach (Phase 2) for item reduction and assessment of the tool's psychometric properties.

The Institutional Ethics Committee for Human Research in Government College of Nursing, Medical College, Thiruvananthapuram, approved the study: CNT/IEC/16/01/14. The study participants wrote written informed consent.

Phase 1

We formulated a conceptual model based on the WHO definition of elder abuse: "a single/repeated act of appropriate action, occurring within any relationship where there is an expectation of trust, which causes harm or distress to an older person."[12] It can take various forms such as financial, physical, psychological, sexual, and neglect.

Item generation was done using deductive and inductive methods. The potentially essential items were initially identified from existing instruments, extensive literature reviews, expert opinions, elder abuse theories, and qualitative data collection methods. Qualitative methods such as FGD and IDI were adopted using the purposive sampling method, with data redundancy determining the sample size. FGD guides and separate IDI guides were prepared for different stakeholders. IDI was done with the help of an interview guide, and probing was done judiciously. All interviews were audio-recorded. The duration of each interview was about 45–60 min.

For FGD, a group of older adults above the age of 60 years were selected with the help of community heads, and Accredited Social Health Activist (ASHA) is a community health worker. We conducted ten FGDs (rural male, rural female, rural mixed gender, urban male, urban female and urban mixed gender, coastal male, coastal female, slum mixed gender, and slum female) with an average number of 8–10 members in each group. The study purpose, voluntary participation, the privacy of information, and the anonymity of the participants were explained. After giving the participant information sheet, verbal and written consent was obtained to participate and audio record the interview.

All interviews were transcribed with special attention and subjected to qualitative analysis such as free-listing, pile sorting, and domain identification. Investigator's review was the first step in item selection and eliminated the items which are duplicated, culturally irrelevant, and overlapped. Next, a panel of experts (two gerontologists, two sociologists, a geriatrician, a psychologist, a nurse working in a geriatric unit, and an epidemiologist) did the item paneling. The experts were requested to rate the relevance of the items on a four-point ordinal scale: one (not relevant), two (somewhat relevant), three (quite relevant), and four (highly relevant). For calculating the item-content validity index (I-CVI), the scale was dichotomized by combining those items with a score of three and four together (relevant) and two and one together (not relevant). Then, I-CVI for each item was computed as the number of experts giving a rating of relevance divided by the total number of experts. The item with I-CVI greater than 79% was considered appropriate, between 70% and 79% needed revision, and those with less than 70%, were eliminated.[13] The endorsement pattern used a three-point Likert scale to best capture the forms of elder mistreatment.

A panel of two bilingual and two subject experts did the forward and backward translation of the 34-item draft tool. The items conceptual, content, semantic, operational, and functional equivalents were maintained during the translation procedure.

A series of pretesting was done to establish the face validity and content validity. Five nursing professionals did peer review to ensure readability, style, formatting, and clarity of language. Experts in gerontology reviewed to ensure the content coverage, clarity, and simplicity of items in the tool. The translated tool was given to the respondent population (10 older men and 10 older women) to test the wording and comprehensibility.

A pilot study was done using purposive sampling of 50 older persons to determine the clarity of items and the time for completion. After minor refinement, we further validated the 34-item draft tool. An additional cognitive interview was done among the 10 elderly who underwent the pilot study to know whether the questions were understood the way they were intended. We estimated test–retest reliability by administering it to 20 elderly twice at an interval of 2 weeks to evaluate the tool's stability over time. The inter-observer reliability of the 34-item draft tool was administered and determined on 20 elderly by a nurse educator and a social worker on the same day. The scores were correlated using intraclass correlation coefficients (ICCs) before the validation phase. Internal consistency reliability was done along with the main study in Phase 2.

Phase 2

The sample size of 344 subjects for the 34-item draft tool for validation was calculated based on the subject-to-item ratio of 10:1.[14] We used the multistage sampling method till ward selection. Subsequently, the selection of elderly 60 years and older was done by cluster sampling from wards. The researcher, accompanied by an ASHA, did a door-to-door survey. The first

house in each cluster (ward was considered the basic unit of cluster sampling) from the voter's list was selected by simple random sampling using the lottery method. The remaining houses were selected by consecutive sampling. While the researcher collected data through a face-to-face interview with the elders, the ASHA engaged the other family members. Only one elderly was selected from each household and was considered a respondent. The researcher obtained written consent from all participants before collecting data.

Statistical analysis

Data were entered in Excel format and were analyzed using the software Statistical Package for the Social Sciences IBM SPSS Statistics Version 25, developed by IBM Corporation, (Armonk, New York, United States). We carried out the descriptive statistics of all variables. The sequential step in the tool development is given in Figure 1.

The following reliability estimations were performed: test–retest and inter-observer reliability using the ICC statistics and internal consistency reliability using Cronbach's alpha coefficient.

Validity analysis

Face and content validity were ensured during the different stages of tool development. Item analysis was used to "clean up" items to maximize each item's reliability and validity. Item analysis included descriptive statistics, correlation matrices, internal consistency (Cronbach's alpha), and factor analysis (for item reduction). Construct validity was established using exploratory factor analysis (EFA). Kaiser–Meyer–Olkin (KMO) measure and Bartlett's test of sphericity were used to determine the suitability for factor analysis. Principal component analysis (PCA) was used to extract the components. PCA yields commonalities, eigenvalues, percentage variance, and component loadings of selected items on the final tool. Communalities of more than 0.4 were taken as a criterion for retaining the items. If an item loads on two or more components, it was considered under the component in which it loaded higher.

The further analysis excluded the item loading greater than 0.35 into a component that did not match the theory and logic. There should be a minimum of two or three items to consider as a component. Varimax rotation was done on the extracted and retained components, which helped better interpretation. Convergent validity was done along with prevalence estimation on another sample of 700 using the Malaysian Elder Abuse Scale (MEAS).[15] This tool is available in the public domain used for the assessment of elder abuse in a domestic setting with a total of 10 items under physical, psychological, and financial abuse domains.

Results

An 80-item pool was generated by IDIs, FGDs, and literature reviews. From this 80-item pool, we selected 49 items after removing the duplicated items and putting these items under the physical, financial, sexual, and psychological abuse domains. We identified subdomains under psychological abuse, namely lack of freedom, isolation, disrespect, and verbal abuse. Expert paneling was done, and items with I-CVI less than 70 were deleted. The items were condensed from 49 to 34 items.

Thirty-four item tools had 23 items in the psychological domain, 5 in the financial domain, and 6 in the physical domain. As per expert opinion, the single item in the sexual domain was reallocated to the physical domain.

Test–retest reliability

ICC of the 34-item draft tool (ICC: 0.94 [confidence interval (CI): 0.9–0.97]) and the inter-observer reliability (ICC: 0.94 [CI: 0.89–0.97]) was calculated.

The 34-item draft tool was administered to 344 elderly subjects for item analysis to establish psychometric properties. Initially, the 34-item tool was analyzed to see descriptive statistics. The average age of the participants was 69.6 (standard deviation = 6.3) years, with half of the respondents being females (54%). A high proportion of the elderly, 45%, had 10 years of schooling, 40.4% had more than 10 years of schooling, 13.4% had less than 7 years, and 1% was illiterate. Regarding economic dependency, 57.2% of the elderly were economically dependent on their children, 9.58% on their spouse, 4.14% on relatives, and 29% were independent.

We deleted the following four items with maximum skewness (>98%): "Has anybody forged your signature in financial transactions? Has anyone tried to choke you to death? Have you ever been scorched? Have you ever been molested?."

A correlation matrix was done on the 30-item tool for the physical, psychological, and financial domains. The following four items with inter-item and item-total scores <0.2 were deleted all under the psychological domain: "Are you restricted from expressing your grievance/addressing your problem in the family or others? Are you restricted to using telephone/mobile? Do you have ample freedom to meet your spiritual needs? Are you allowed to accompany family members for social/religious functions (like marriage/funeral/temple/church)?."

The internal consistency reliability of Cronbach's alpha of the 26 items was 0.93. We did EFA. The KMO value derived for the tool was 0.88, and Bartlett's test of sphericity rejected the null hypothesis ($P < 0.001$). All items in the 26-item tool had communality >0.5. The PCA yielded four components with eigenvalue >1 with a cumulative variance of 69.6%. After a series of rotations, 11 items were deleted. An item's selection or deletion becomes more sensible if done on rotated solutions.

All items (15) in the final tool had communality >0.5 and were again subjected to PCA. PCA generated four components with eigenvalue >1 with a cumulative percent variance of 72.4%.

The Scree plot of the final 15-item tool showed a steep downward slope to become a horizontal line at 1.5, which yielded four components [Figure 2]. Varimax rotation, which is an orthogonal rotation, further confirmed four components. We

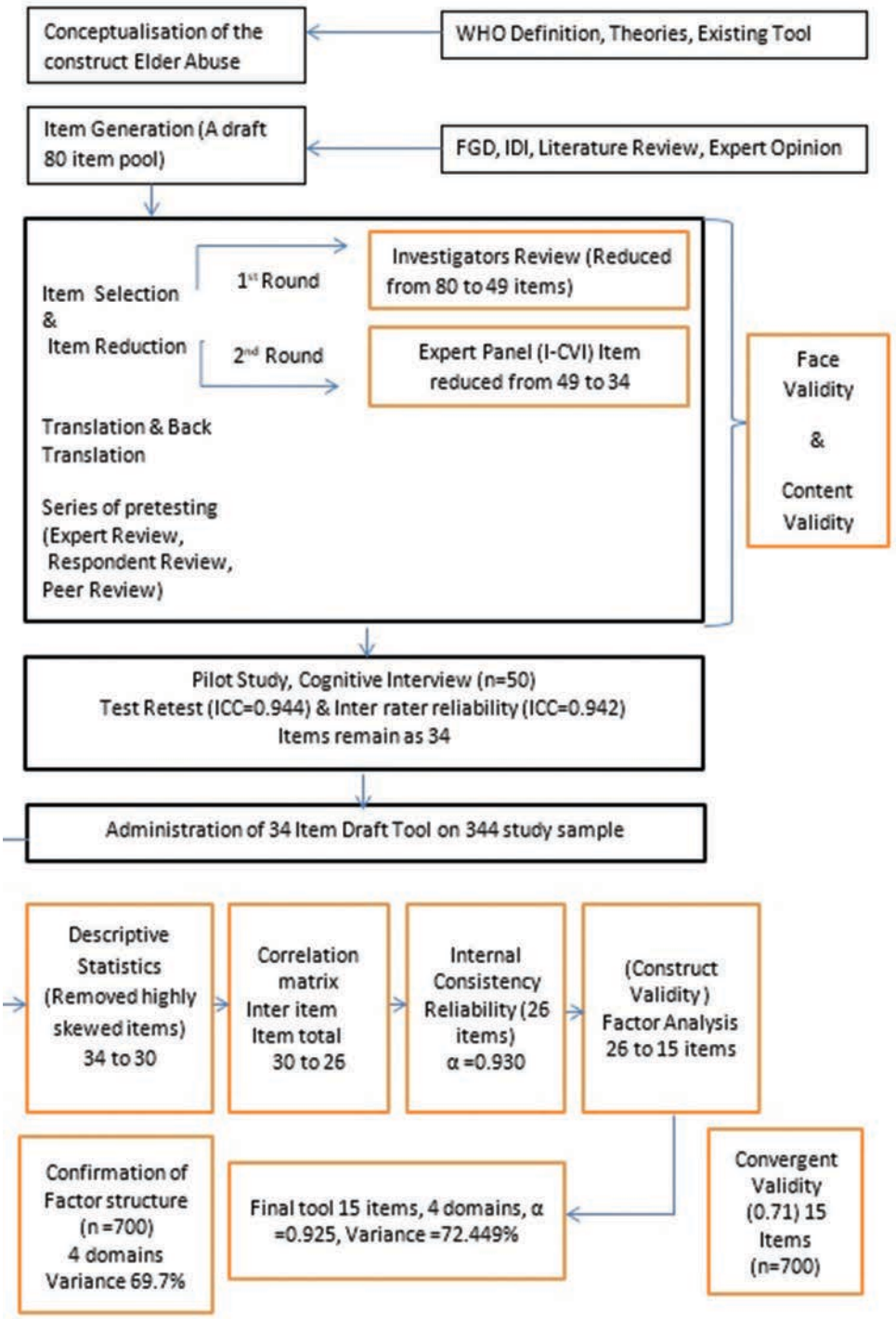

Figure 1: Flowchart of sequential steps in the development of elder mistreatment screening tool. FGD: Focus group discussion, IDI: In-depth interview, I-CVI: Item-content validity index, ICC: Intraclass correlation coefficient

named the four components as verbal abuse (5 items), neglect (4 items), physical abuse (3 items), and financial abuse (3 items):

1. Component 1: "Verbal abuse" items accounted for 22.9% of the total variance. This component includes five items and reflects verbal acts, with the highest loading item of 0.79 to the lowest of 0.62
2. Component 2: "Neglect" items accounted for 17.8% of the total variance. This component includes four items depriving the elderly of the needed services and leaving the elderly at risk (the highest component loading of 0.74 and the lowest of 0.55)
3. Component 3: "Physical abuse" items accounted for 17.2% of the total variance. This component includes three items about the intentional use of physical force that distresses the elderly (the highest loading item of 0.85 to the lowest of 0.75)

4. Component 4: "Financial abuse" items accounted for 14.3% of the total variance. This component includes three items about the improper use of an older individual's resources by a caregiver (the highest loading item of 0.76 to the lowest of 0.69).

We named the new tool as Elder Mistreatment Screening Tool (EMST) [Table 1]. The total score of EMST ranges between 0 and 30, with three negatively scored items.

The Pearson correlation between the EMST and the MEAS was 0.719 ($P < 0.001$). This was done on a 700 sample to estimate the prevalence of elder mistreatment.

Discussion

We present the development and validation of a culturally and linguistically appropriate and psychometrically robust screening tool (EMST) for elder abuse. The tool development process followed the recommendations by the Nunnally protocol and the COnsensus-based Standards for the selection of health Measurement INstruments.[14] This process included two phases: in Phase 1, a 34-item draft tool was developed by deductive methods (extensive literature review and preexisting scales) and inductive methods (FGD with the target population and IDI with different stakeholders). This draft tool was revalidated through peer and expert reviews, assessed comprehensibility through a pilot study followed by test–retest and inter-rater reliability. We used I-CVI to select the most appropriate items from the items generated.[13] Even though we conceptualized using a five-point Likert scale for finer gradation; we found this response format confusing for our population and finally adopted a three-point Likert scale. In Phase 2, we establish the psychometric properties of the tool.

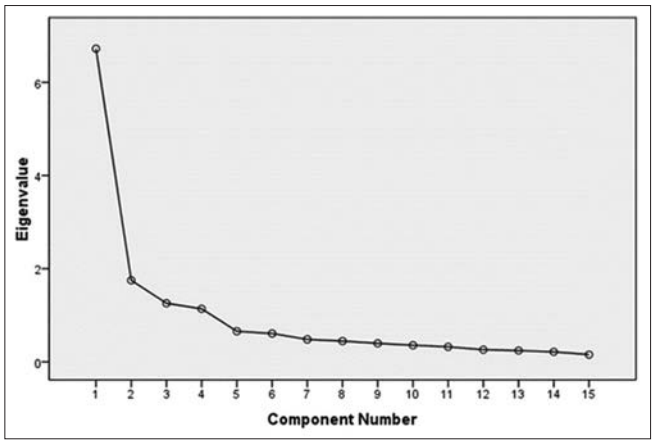

Figure 2: Scree plot

The final 15-item EMST under four components could explain a total variance of 72.4%, above the desired level of 60%.[16] It also had good internal consistency ($\alpha = 0.92$) which falls under four distinct domains. A good correlation with the MEAS ($P < 0.001$) showed that EMST measured the same concepts.

We confirmed the same four components by repeating factor analysis in a separate 700-subject sample in a community setting along with a prevalence study. This strengthens the notion that it is a valid research tool for screening elder abuse in family settings.

The final components derived, namely physical, financial, verbal, and neglect, were similar to our hypothesized components, except for sexual abuse. Studies in India have reported the same components, with neglect and verbal abuse being the most reported, followed by financial and physical abuse.[17,18] The reason for sexual abuse not emerging as an

Table 1: Elder Mistreatment Screening Tool

		During the last year		
Item number	**Items**	**Most of the time**	**Sometimes**	**Never**
1.	Do the family members curse you/use abuse words in front of others?	2	1	0
2.	Do family members shout at you for silly matters?	2	1	0
3.	Are you threatened to be thrown out of house?	2	1	0
4.	Have you been asked to seek another place of living?	2	1	0
5.	Has any family member expressed his/her desire that you were dead?	2	1	0
6.	Do family members inform you about family matters	0	1	2
7.	Have you been asked silent in the house by anyone in the family?	2	1	0
8	Do family members take proper care of you in the event of hospitalization?	0	1	2
9	Do you get adequate amount of food in time?	0	1	2
10	Have you been hit/kicked/slapped?	2	1	0
11	Have anyone thrown objects that are harmful to you?	2	1	0
12	Has anyone tried to restrain within the house?	2	1	0
13.	Have you ever been forced to sign documents related to properties belonging to you?	2	1	0
14.	Have you been denied protection by family members after acquiring your protection?	2	1	0
15.	Were there any instant of arguments related to property matters?	2	1	0

Total score: Psychological abuse: 1–5 questions, Neglect: 6–9 questions, Physical abuse: 10–12 questions, Financial abuse: 13–15 questions. Scoring pattern: Most of the time: 2, Sometimes: 1, Never: 0. Total score ranges between 0 and 30. Score reversal in items: 6, 8, and 9, Abused: Score ≥1, Not abused score=0

essential factor in EMST may be attributed to lack of disclosure rather than its absence.

Due to the nonavailability of culturally appropriate and locally validated community screening tools, studies from India utilized tools such as the Hwalek-Sengstock Elder Abuse Screening Test (HS/EAST) and Vulnerability Abuse Screening Scale (VASS) developed elsewhere, primarily developed for screening risk factors for elder abuse.[19,20] The HS/EAST can identify the three forms of abuse, namely violating personal rights, vulnerability, and abusive situations. The scale scored low reliability of Cronbach's alpha 0.29. VASS was developed to identify the risk of abuse among older women. The items for this scale were adopted from H-S/EAST and Conflict Tactics Scale. The internal consistency of the overall tool was only 0.4, sharing a total variance of 51%. In contrast, EMST has been developed by giving significance to the elderly individual and emphasizing their perception as a significant factor in identifying the domains and generating items based on it.

The two commonly used scales to screen for elder abuse in community settings are the Geriatric Mistreatment Scale (GMS) and the MEAS.[21] The GMS with an initial item pool of 49 items was generated from a consensus of a survey expert group. After item reduction, 22 items of GMS were obtained, which measure physical, psychological, financial, neglect, and sexual abuse. The Cronbach's alpha was 0.83 with a response format of yes/no.

MEAS items were initially identified from published tools, literature reviews, and elder abuse theories. Cronbach's alpha for the total scale was 0.62. The limitations include only three factors (physical, psychological, and financial), test–retest reliability not being estimated, the yes/no response format, and the low overall variance of 59.4%.

Limitation

Due to the absence of a gold standard tool, we could not estimate the sensitivity, specificity, negative predictive value, and positive predictive value of EMST.

Conclusion

The newly developed EMST is a short, simple, interviewer-administered screening instrument. The final 15-item tool could explain 72.4% of the variance of 30 theoretically identified possible items when used on a sample of 344 elderly persons. A respondent is categorized as abused with the presence of a single item indicating abuse. As the EMST shows evidence of satisfactory reliability and validity, this screening tool can be used to assess elder abuse in family settings.

Financial support and sponsorship

Nil.

Conflicts of interest

There are no conflicts of interest.

References

1. Katttakayam JJ. Post retirement adaptation of elderly in Kerala, India. Innov Aging 2017;1 Suppl 1:126.
2. Baker MW. Elder mistreatment: Risk, vulnerability, and early mortality. J Am Psychiatr Nurses Assoc 2007;12:313-21.
3. Dong X, Simon MA. Elder abuse as a risk factor for hospitalization in older persons. JAMA Intern Med 2013;173:911-7.
4. Lachs MS, Williams CS, O'Brien S, Pillemer KA, Charlson ME. The mortality of elder mistreatment. JAMA 1998;280:428-32.
5. Jamuna D. Issues of elder care and elder abuse in the Indian context. In: An Aging India: Perspectives, Prospects, and Policies. New York: Routledge; 2013. p. 125-42.
6. Prakash IJ. Elder abuse: Global response and Indian initiatives. Indian J Soc Work 2001;62:446-63.
7. Saikia AM, Mahanta N, Mahanta A, Deka AJ, Kakati A. Prevalence and risk factors of abuse among community dwelling elderly of Guwahati City, Assam. Indian J Community Med 2015;40:279-81.
8. Sebastian D, Sekher TV. Abuse and neglect of elderly in Indian families: Findings of elder abuse screening test in Kerala. J Indian Acad Geriatr 2010;6:57-9.
9. Reingle Gonzalez JM, Cannell MB, Jetelina KK, Radpour S. Barriers in detecting elder abuse among emergency medical technicians. BMC Emerg Med 2016;16:36.
10. Yon Y, Mikton CR, Gassoumis ZD, Wilber KH. Elder abuse prevalence in community settings: A systematic review and meta-analysis. Lancet Glob Health 2017;5:e147-56.
11. Abolfathi Momtaz Y, Hamid TA, Ibrahim R. Theories and measures of elder abuse. Psychogeriatrics 2013;13:182-8.
12. Mysyuk Y, Westendorp RG, Lindenberg J. Added value of elder abuse definitions: A review. Ageing Res Rev 2013;12:50-7.
13. Zamanzadeh V, Ghahramanian A, Rassouli M, Abbaszadeh A, Alavi-Majd H, Nikanfar AR. Design and implementation content validity study: Development of an instrument for measuring patient-centered communication. J Caring Sci 2015;4:165-78.
14. Nunnally JC. An overview of psychological measurement. In: Clinical Diagnosis of Mental Disorders.: A handbook. Springer: Boston; 1978. p. 97-146.
15. Hamid TA, Momtaz YA, Ibrahim R, Mansor M, Samah AA, Yahaya N, *et al*. Development and psychometric properties of the Malaysian elder abuse scale. Open J Psychiatry 2013;3:283-9.
16. Streiner DL, Norman GR, Cairney J. Health Measurement Scales: A Practical Guide to Their Development and Use. Oxford University Press, UK; 2015.
17. Chokkanathan S, Lee AE. Elder mistreatment in urban India: A community based study. J Elder Abuse Negl 2005;17:45-61.
18. Srinivas S, Vijayalakshmi B. Abuse and neglect of elderly in families. Indian J Soc Work 2001;62:464-79.
19. Özçakar N, Toprak Ergönen A, Kartal M, Baydur H. Adaptation, reliability, and validity study of the Hwalek-Sengstock Elder abuse screening test (H-S/EAST): A Turkish version. Turk J Med Sci 2017;47:1894-902.
20. Schofield MJ, Mishra GD. Validity of self-report screening scale for elder abuse: Women's health Australia study. Gerontologist 2003;43:110-20.
21. Giraldo-Rodríguez L, Rosas-Carrasco O. Development and psychometric properties of the geriatric mistreatment scale. Geriatr Gerontol Int 2013;13:466-74.

Original Article

Morin Modulates the Activities of Pro-inflammatory Enzymes and Expression of Cytokines and Nuclear Factor Kappa B in the Heart, Liver, and Pancreas in Streptozotocin-induced Diabetic Rats

Simon Monisha Nirmala, Mini Saraswthy

Department of Biochemistry, University of Kerala, Karyavattom, Thiruvananthapuram, Kerala, India

Abstract

Background: Persistent diabetes leads to inflammatory changes in liver, heart, and pancreas resulting in pathological alterations. Morin's ability to reduce inflammation in the pancreas, liver, and heart of streptozotocin (STZ)-induced diabetic rats was assessed. **Methods:** Male Sprague–Dawley rats were given a single intraperitoneal injection of STZ at a dose of 40 mg/kg body weight to develop diabetes. Morin (50 mg/kg b. wt) and metformin (100 mg/kg) were given orally for 45 days. Proinflammatory enzymes such as myeloperoxidase, nitric oxide synthase, lipoxygenase, and cyclooxygenase were analyzed. Expressions of interleukin (IL)-6, (TNF-α), and nuclear factor kappa B (NF-κB) in the heart, liver, and pancreas were also studied. Data were statistically analyzed. **Results:** Blood glucose and glycosylated hemoglobin levels significantly decreased in the treated groups. The activity of proinflammatory enzymes which were increased in the diabetic rats was reduced significantly when treated with morin and metformin. The expression of NF-κB, TNF-α, and IL-6, of heart, liver, and pancreas showed significant downregulation in the morin treated groups in comparison with diabetic control rats. The findings of histopathological analysis suggest that morin is a promising compound in the diabetic studies. **Conclusion:** Morin reduced the levels of inflammatory enzymes, glucose, and HbA_1C. The STZ-induced diabetic rats exhibited the increased expression levels of proinflammatory cytokines and NF-κB in the heart, liver, and pancreas, which were significantly reduced by morin and metformin.

Keywords: Cytoprotection, diabetes, inflammation, metformin, morin, proinflammatory cytokines

Introduction

The type 2 diabetes (T2DM) incidence is increasing worldwide and more prevalent in middle-income countries. T2DM induces significant inflammatory changes in the liver, heart, and pancreas, contributing to disease progression and complications. Chronic hyperglycemia triggers oxidative stress, initiating nuclear factor kappa B (NF-κB) and MAPK signaling activation. Diabetes causes steatohepatitis in the liver, which is typified by elevated tumor necrosis factor-alpha (TNF-α) and interleukin-6 (IL-6) levels as well as immune cell infiltration. Cardiac inflammation in diabetes is associated with endothelial dysfunction, fibrosis, and upregulation of adhesion molecules, leading to diabetic cardiomyopathy. The pancreas experiences β-cell dysfunction due to inflammatory cytokines, impairing insulin secretion and accelerating disease progression. Targeting inflammatory pathways is a promising strategy for managing diabetes-related organ damage. According to earlier research, transcription factors, nuclear receptors, cell surface receptors, and their coregulators are just a few of the many levels at which these processes are regulated.[1] Insulin resistance is linked

Access this article online

Quick Response Code:

Website: https://journals.lww.com/hrcm/

DOI: 10.4103/JHCR.JHCR_3_25

Address for correspondence: Prof. Mini Saraswthy, Department of Biochemistry, University of Kerala, Karyavattom, Thiruvananthapuram - 695 581, Kerala, India.
E-mail: minisaraswthy@gmail.com

Received: 03-03-2025 **Revised:** 20-04-2025
Accepted: 20-04-2025 **Published:** ***

How to cite this article: Nirmala SM, Saraswthy M. Morin modulates the activities of pro-inflammatory enzymes and expression of cytokines and nuclear factor kappa B in the heart, liver, and pancreas in streptozotocin-induced diabetic rats. J Adv Health Res Clin Med 2025;XX:XX-XX.

to serine/threonine phosphorylation, which governs insulin receptor signaling.[2] By activating serine kinases such as IκB kinase β c-Jun N-terminal kinase, ribosomal protein S6 kinase, and mammalian target of rapamycin 32 in adipocytes, pro-inflammatory cytokines secreted by macrophages (IL-1 β, IL-6, and TNFα) can cause inhibitory phosphorylation, which in turn causes insulin receptor substrate 1 to become insulin resistant (IR).[3] Therefore, inflammation and activated immunity play important roles in the etiology of diabetes.[4,5] The study in rodents demonstrated that eicosanoids from arachidonic acid modulate inflammatory cytokines and chemokines and contribute to the pathogenesis of IR- and T2DM-associated complication.[6]

The WHO suggest the evaluation of traditional plants with hypoglycemic potential may lead to novel antidiabetic moieties.[7] Phytoconstituents such as alkaloids, polyphenols, flavonoids, coumarins, and triterpenoids were reported to possess antidiabetic potential to treat diabetes and associated complications.[8] A naturally occurring bioflavonoid, morin was identified from the members of the *Moraceae* family and is present in a variety of fruits and herbs, including red wine, mulberries, onions, guavas, almond, fig, and mill. Previous studies suggest the useful effect of Morin on some human diseases. Morin has systemic protective action, the potential to reduce side effects of drugs, without affecting their functions. This compound's favorable safety profile makes it a viable contender deserving of more research.[9] The present study investigated the anti-inflammatory potential of morin in experimental diabetes mellitus.

Materials and Methods

Chemicals

Biochemicals were purchased from Sigma Aldrich (St. Louis, MO, USA), Merck Chemical Company (Darmstadt, Germany) and Sisco Research Laboratories (Mumbai, India). Commercially purchased morin (Sigma-Aldrich, CAS No. 654055-01-3, Product No. M4008), with a purity of ≥ 85% (high-performance liquid chromatography) was used.

Experimental animals

Male Albino rats of the same breed (mean body weight of 250 g) were used as the experimental model system. The animals were bred and kept in the animal house, Department of Biochemistry, University of Kerala. They were housed in polypropylene cages under the standard environmental conditions (25 ± 10°C; 12 h light/dark cycle) with food and water *ad libitum*. Institutional ethics committee approved the studies [IEAC-KU-7/2015-16-BC-SM (25)].

Induction of diabetes

Animals were divided into five groups with eight rats each. Group I, Normal (N); Group II, Normal + Morin (N + Mo) (50 mg/kg), Group III, Diabetic control (D), Group IV, Diabetic + Morin (D + Mo) (50 mg/kg), Group V, Diabetic + Metformin (D + Met) (100 mg/kg). A single intraperitoneal injection of newly made streptozotocin (STZ) (40 mg/kg) in 0.1 M citrate buffer (pH 4.5) caused rats to develop diabetes. The animals were allowed to drink 5% glucose solution overnight to overcome the drug-induced hypoglycemia. If the animals' blood glucose levels were more than 250 mg/dl on the third day after receiving a STZ injection, they were classified as diabetics. The doses of morin selected based on the previous study.[10] On the third day of the STZ injection, which was regarded as the beginning day of treatment, the Morin and Metformin regimen was initiated. The course of treatment lasted for 45 days.

Determination of blood parameters

Hugget and Nixon's glucose oxidase technique was used to estimate the blood glucose levels.[11] A Beacon Diagonostics Pvt. Ltd. kit from India was used to assess glycated hemoglobin.[12] The activities of inflammatory marker enzymes were assayed in the plasma collected from the heparinized blood. Assay of cyclooxygenase (COX) by TBA method.[13] Lipoxygenase (LOX) by Axelrod and Hogan.[14] Total nitric oxide synthase (NOS) by Salter and Knowles[15] and myeloperoxidase (MPO) by the method described by Bradley *et al*.,[16] Protein was measured using the Lowry *et al*. technique.[17]

Determination of gene expression using the reverse transcription polymerase chain reaction

TRIZOL Reagent (Sigma Aldrich) was used to isolate total RNA from the liver, heart, and pancreas using the technique outlined by Chomczynski and Mackey.[18] To investigate the expression of IL-6, TNF-α, and NF-κB, the extracted RNA was subjected to reverse transcription polymerase chain reaction (RT-PCR). Using a cDNA synthesis kit (Fermentas, Vilnius, Lithuania), omniscript RT reverse-transcribed 2 mg of total tissue RNA after priming it with 0.05 mg of oligodT [Table 1]. Among these, the RNA primer was made by mixing oligo dT and random hexamer in a 3:1 ratio. Depending on the RNA concentration of the sample, the final volume was changed to obtain 500 ng of RNA. A centrifuge was used to thoroughly combine and spin the reaction mixture. After an hour of incubation at 42°C, the reaction was halted by heating it for 5 min at 95°C. MgCl2 (4 mM), a reaction buffer, dNTP (dGTP, dCTP, dTTP, and dATP) at 0.4 mM each, and Taq DNA polymerase (0.05 U/μl) made up the PCR master mix utilized for the RT-PCR procedure. In the prescribed order,

Table 1: Preparation of cDNA synthesis reaction mixture

Components	Volume (μL)	Final concentration
5X cDNA synthesis buffer	4	1X
DNTP mix	2	500 μm each
RNA Primer	1	
RT enhancer	1	
Verso enzyme mix	1	
Template (RNA)	1–5	1 ng
Water, nuclease-free	Up to 20	
Total volume	20	

RT: Reverse transcriptase, DNTP: Deoxynucleoside triphosphates

the reagents were pipetted into a sterile, nuclease-free tube and stored in ice [Table 2]. The test system underwent PCR under the following thermal cycling conditions: primer annealing at 58°C (50°C–65°C) for 30 s, primer extension at 72°C for 45 s, and template denaturation at 95°C for 15 s.

An Eppendorf thermocycler (model 5332) was used to do PCR. Table 3 provides primer sequences. For 35 cycles, PCR was carried out using a mixture of PCR buffer, 25 mM MgCl2, 5U Fermentas DNA polymerase, 3 µl cDNA, and 20 pmol of each primer. Quantity One imaging software (BioRad) was used to normalize the amplified product (100 ng) against an internal control, GAPDH, after it had been electrophoresed on a 1% agarose gel containing ethidium bromide and subjected to densitometric scanning (BioRad Gel Doc) to ascertain each gel's optical density.

Histopathological analysis of the liver and pancreas

The liver, heart, and pancreas from each experimental group were collected in 10% formalin solution and immediately processed by the paraffin technique. Thin sections (5 µm) were cut and stained with hematoxylin and eosin. The tissue samples were then examined and photographed under a light microscope.[19]

Statistical analysis

Statistical analysis was done as described by Bennet and Franklin.[20] All analysis were performed on computer using the statistical package SPSS. Data were analyzed by one-way analysis of variance (ANOVA). Data expressed as mean value ± SD. Comparisons between the groups were made by Duncan's Multiple Range Test. '*p*' less than 0.05 was significant.

Results

Level of glucose and HbA_1C

Table 4 displays the blood glucose and blood HbA1C percentage. Compared to the normal control (N) and normal rats treated with morin (N + Mo) groups, the diabetic control group (D) had significantly ($P < 0.05$) higher blood glucose and HbA1C values. In diabetic rats, the addition of metformin and morin dramatically lowered the HbA1C and glucose levels.

Table 2: Reaction mixture for reverse transcriptase polymerase chain reaction

Components	Volume
PCR Master Mix (2X)	25 µL
Forward primer	0.1–1.0 µm
Reverse primer	0.1–1.0 µm
Template DNA	10 pg–1 µg
Water, nuclease-free	50 µL
Total volume	50 µL

PCR: Polymerase chain reaction

Pro-inflammatory enzymes analysis

Compared to the normal group, the diabetic control rats had considerably higher levels of COX, 5-LOX, 15-LOX, NOS, and MPO activities, whereas the normal rats treated with morin showed a significant decrease in these activities. When compared to the diabetic control group, diabetic rats treated with morin and metformin displayed decreased activity.

In diabetic rats, metformin therapy had a greater impact on the inflammatory markers than morin. The graphs in Figure 1a-e, respectively, display the activity of COX, 5-LOX, 15-LOX, NOS, and MPO.

Pro-inflammatory cytokines and nuclear factor kappa B expressions in heart, liver, and pancreas

When compared to the N and N + M groups, the diabetes group's heart, liver, and pancreatic mRNA expressions of the pro-inflammatory cytokines TNF-α and IL-6 were considerably ($P < 0.05$) up-regulated. In comparison to the normal control, many pro-inflammatory genes were markedly downregulated in the N + M group. Treatment with morin and metformin significantly ($P < 0.05$) decreased these genes in diabetic rats. The N + M group and the normal control groups had similar levels of NF-κB expression in the heart, liver, and pancreas. However, compared to normal groups, its expression was considerably ($P < 0.05$) higher in the diabetes group. In diabetic rats, the mRNA expression of NF-κB was dramatically ($P < 0.05$) reduced by supplementing with morin and metformin. Figure 2 depicts the expressions in a, b, and c.

Histopathological studies

Histopathological studies of diabetic rat liver showed degeneration of hepatocytes, distorted portal vein and necrosis of parenchyma cells [Figure 3]. Inflammation was evident. Liver of normal rats showed normal hepatocytes with no degeneration. Inflammation was absent in normal rats. Morin and metformin supplemented diabetic rats showed a near normal morphology with mild degeneration of hepatocytes when compared to normal rats.

Histopathological findings of pancreatic tissue revealed severe necrosis and atrophy of islets in diabetic rats [Figure 4]. Normal rats showed tightly arranged islets with no degeneration, while the pancreas of Morin supplemented normal rats showed

Table 3: Rat-specific polymerase chain reaction primer sequences

Gene	Forward primer	Reverse primer	Accession number
TNF-α	5'-TTGCTTCTTCCCTGTTCC-3'	5'-CTGGGCAGCGTTTATTCT-3'	AY427675.1
IL-6	5'-CTTCCAGCCAGTTGCCTTCT-3'	5'-GACAGCATTGGAAGTTGGGG-3'	NM012589.1
NF-κB	5'-CCTAGCTTTCTCTGAACTGCAAA-3'	5'-GGGTCAGAGGCCAATAGAGA-3'	U83656.1
GAPDH	5'-CCGTTCAGGTCTGGGATGAC-3'	5'-GGGCAGCCCAGAACATCAT-3'	NM017008.4

IL-6: Interleukin-6

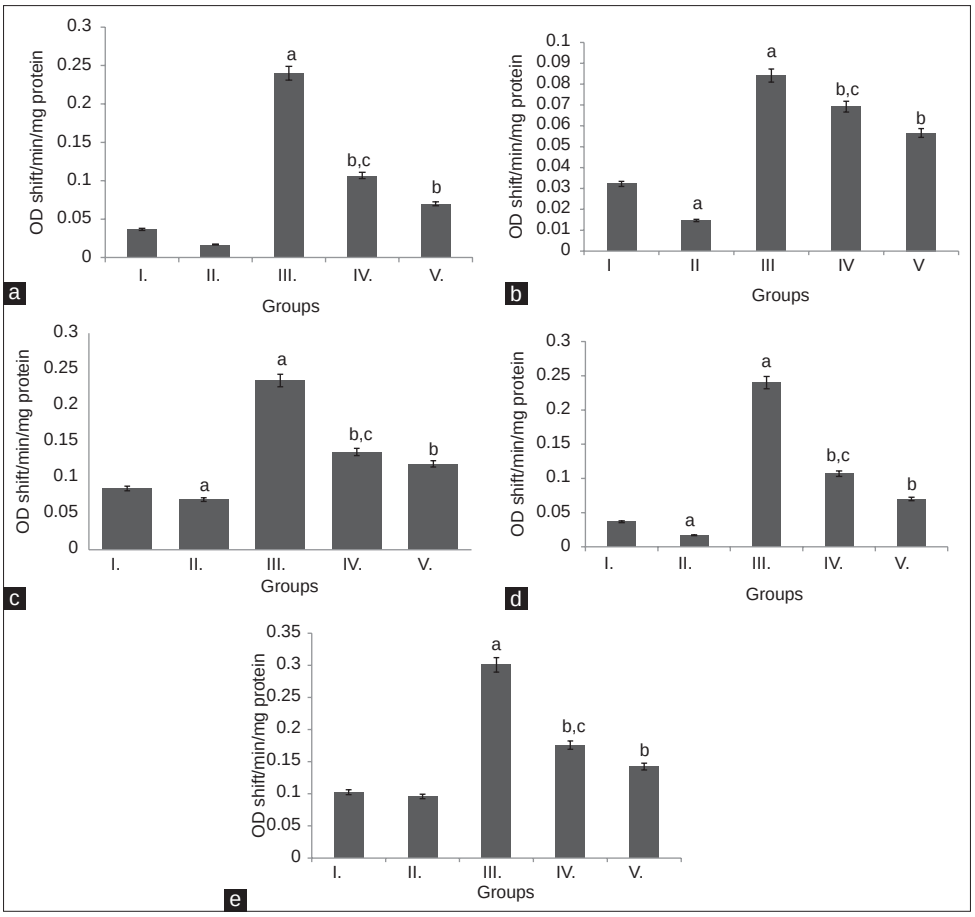

Figure 1: Activity of enzymes in plasma with heparin as anticoagulant. (a) Cyclooxygenase; (b) 5-lipoxygenase; (c) 15-lipoxygenase; (d) Nitric oxide synthase; and (e) Myeloperoxidase. Values are mean ± standard deviation, $n = 8$. Group II– normal + Morin, Group III - diabetic, Group IV - diabetic + Morin, Group V - diabetic + Metformin. "a" indicates values significantly differ from Normal (i). Group I - Normal, Group I have been compared with Groups II and III. "b" indicates values significantly differ from diabetic Group (III), which has been compared with Groups IV and V. "c" indicates the values that significantly differ from Group V. Significance accepted at $P < 0.05$

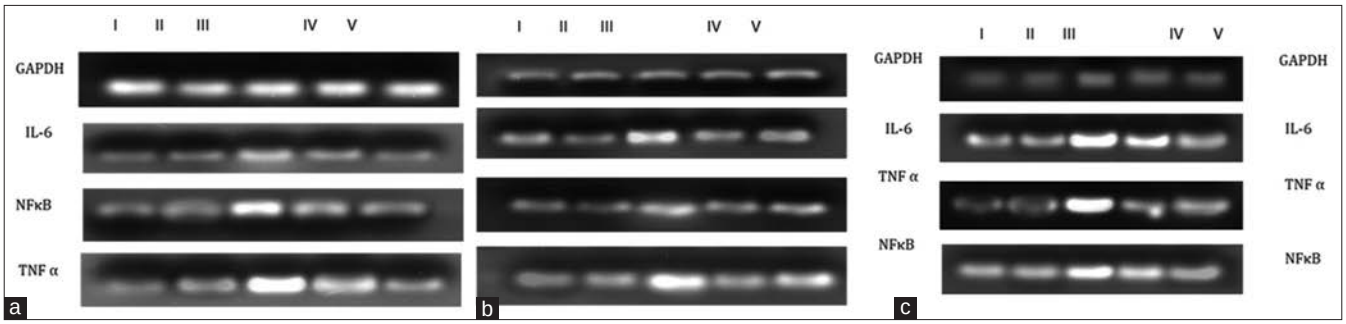

Figure 2: mRNA expression of pro-inflammatory cytokines and nuclear factor kappa B in (a) Heart, (b) Liver and (c) Pancreas. Group I – Normal, Group II– Normal + Morin, Group III - Diabetic, Group IV - Diabetic + Morin, Group V - Diabetic + Metformin

morphology similar to that of untreated normal rats. Only slight necrosis and degeneration were visible in the pancreas of diabetic rats given morin and metformin. The islets' histology revealed morphology that was almost identical to that of typical rats.

Discussion

Flavonoids are gaining considerable attention as therapeutic agents due to their broad-spectrum bioactivities. Morin, a naturally occurring flavonol and dietary polyphenol, exhibits well-documented antioxidant, anti-inflammatory, antihyperglycemic, hepatoprotective, and neuroprotective effects, supported by extensive *in vivo* and *in vitro* studies. Its ability to modulate key biomolecules and biochemical pathways, without interfering with drug action, makes it a promising candidate for combination therapies. Morin has

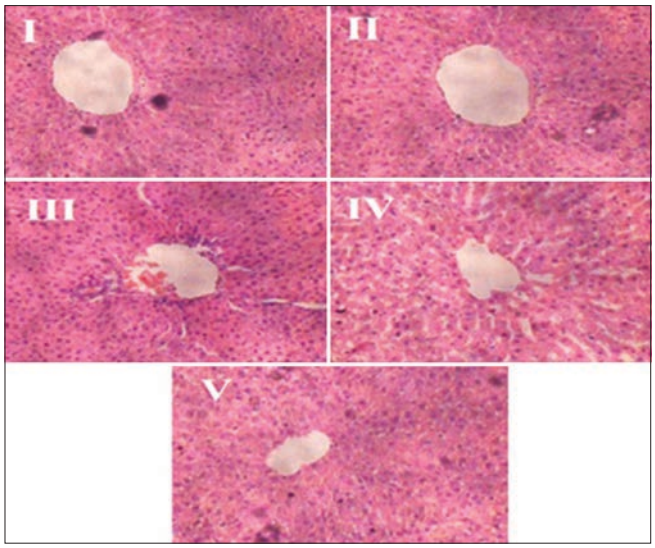

Figure 3: Photomicrograph of liver: Normal rats and Normal + Morin treated normal rats exhibit intact hepatocytes (I and II). Hepatocyte degeneration, distorted portal veins, and parenchymal necrosis with inflammation in diabetic rats (III). Morin-and metformin-treated diabetic rats display nearly normal liver morphology with minimal hepatocyte degeneration. (IV and V). (H and E, ×20)

Table 4: Concentration of glucose and percentage of glycated hemoglobin in blood

Group	Concentration of glucose (mg/dL)	HbA_1C (%)
Normal	93.37±8.88	4.84±0.44
Normal + morin	92.25±8.41	5.64±0.51
D	350.55±31.99a	11.99±1.09[a]
D + morin	153.75±14.03b	9.23±0.84[b,c]
D + metformin	137.35±12.53b	6.86±0.62[b]

[a]Values significantly differ from Normal (I). Group I has been compared with Groups II and III, [b]Values significantly differ from diabetic Group (III), which has been compared with Groups IV (D + morin) and V (D + metformin), [c]Values that significantly differ from Group V. Significance accepted at $P<0.05$. Values are mean±SD, $n=8$. HbA1C: Glycated hemoglobin, D: Diabetic control, SD: Standard deviation

demonstrated significant efficacy in mitigating oxidative stress and age-related diseases, including diabetes, neurodegeneration, and cardiovascular conditions. Prior research conducted in our lab demonstrated that 50 mg/kg body weight of morin has neuroprotective effects and therapeutic benefits in diabetes mice while preserving a favorable safety profile.[10] In this study, morin's anti-inflammatory properties in type 2 diabetes are assessed, along with its effectiveness in comparison to the well-known anti-diabetic medication metformin.

High blood glucose levels in diabetic rats induced by STZ confirmed abnormalities of glucose metabolism. Irreversible damage to the pancreatic beta-cells, which results in degranulation and a loss of insulin secretion capacity, is the direct cause of STZ's diabetogenic activity.[21] Supplementation of Morin significantly reduced the glucose levels significantly in diabetic rats, by the virtue of its antihyperglycemic and insulin mimetic action. The observed effect could be attributed

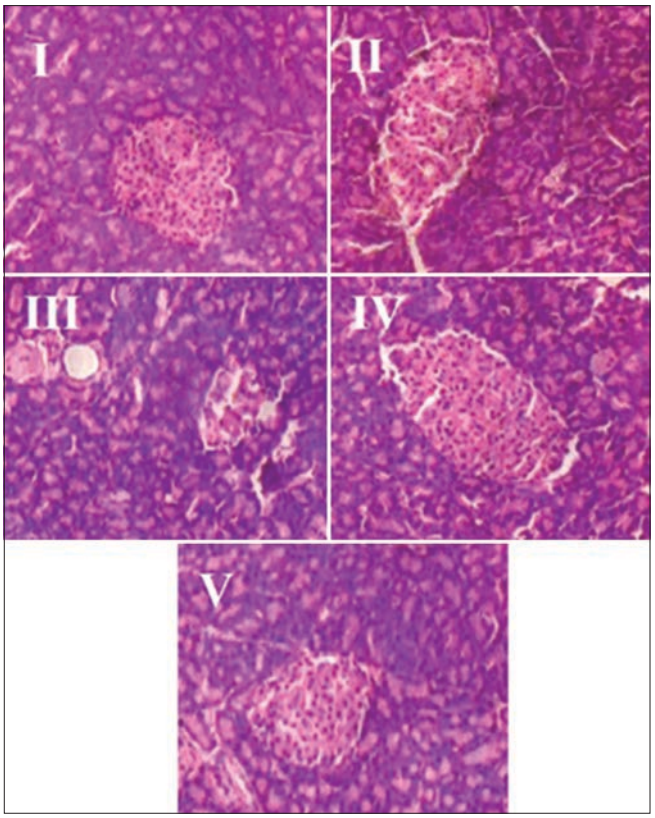

Figure 4: Histopathological analysis of pancreas. Normal and Morin-treated normal rats exhibit intact islet structures (I and II). Diabetic rats show severe islet necrosis and atrophy (III). Morin and metformin supplementation significantly reduced pancreatic necrosis and degeneration, restoring islet morphology to near-normal levels (IV and V). Stained with H and E, ×20

to pancreatic β cell regeneration by morin supplementation. Metformin treatment also led to decreased blood glucose level in diabetic rats. Elevated ROS levels exacerbate tissue damage in liver, heart and pancreas. Pro-inflammatory enzymes, viz, COX-2 and inducible NOS (iNOS) further amplify inflammatory responses, contributing to metabolic dysregulation. Macrophage polarization towards the M1 phenotype in diabetic tissues worsens inflammation and insulin resistance. Fibrosis and apoptosis in these organs further impair their function, increasing susceptibility to complications. Hyperglycemia causes increased activation of inflammatory pathways.[22]

HbA_1C level is an index of the glycemic control and key marker to assess diabetes severity. Diabetic rats of the present study showed higher levels of glycosylated Hb indicating the poor glycemic control in accordance with the results of Mohammed *et al.*,[23] Treatment of Morin has reduced the glycosylated Hb levels and a very notable reduction was shown by metformin in the diabetic group. Increased muscle cell absorption of fatty acids by hyperlipidemia results in the synthesis of fatty acid metabolites, which in turn induce inflammatory cascades and disrupt insulin signalling.

According to Luo and Wang[6] during diabetes, arachidonic acid and its eicosanoid metabolite, significantly contribute to inflammation mediated β-cell dysfunction and insulin resistance. PGE2, a COX product of islets, during cytokine-induced inflammation impairs insulin secretion and insulin sensitivity. Diabetes can exacerbate subsequent inflammatory and vascular events by increasing COX expression and activity in vascular cells and monocytes.[24] Higher COX activity was seen diabetic rats in the present study and the increased COX activity in diabetic condition was significantly reduced in the Morin and metformin treated groups, suggesting their anti-inflammatory effects in diabetic condition.

12-HETE (5-hydroperoxyeicosatetraenoic acid) is a LOX product in islets. Previous reports indicate that LOX pathway contributes to diabetic complications and insulin resistance. Increased levels of 5-LOX and 15-LOX are involved in inflammation and β cell dysfunction.[6] The current study's investigations showed that the diabetic control rats' 5-LOX and 15-LOX levels were much greater than those of the normal rats. But the levels have significantly reduced in morin and metformin supplemented groups, and metformin showed superior effect.

Diabetic rats displayed elevated total NOS activity. Increased NO levels, produced by iNOS, contribute to the pathogenesis and complications resulting from Diabetes mellitus.[25] The groups treated with metformin and morin showed a significant decrease in NO levels. Rats treated with metformin showed significantly lower values than the group treated with morin. One important enzyme that connects inflammation with diabetes is MPO. Olza *et al*. have shown elevated MPO levels in diabetic rats.[26] ROS and other pro-inflammatory mediators are produced by MPO. By intensifying inflammatory processes, its elevated expression and activity in diabetes lead to oxidative stress, insulin resistance, and the emergence of vascular problems. MPO targeting has therapeutic promise for controlling the negative consequences of diabetes. The diabetic group showed a considerable increase in MPO activity, but the metformin and morin supplements considerably decreased MPO activity, with metformin being more effective at lowering MPO activity.

According to Akash *et al*.,[27] even though, various pathogenic responses contribute to insulin resistance through inflammation and impairing insulin secretion from β-cells, hyperglycemia, oxidative stress and dyslipidemia are directly involved in tissue specific inflammation. A number of proinflammatory mediators, including IL-1 β, TNF-α, IL-6, and cytokines and chemokines that are dependent on IL-1, are stimulated by elevated glucose levels. Tissue-specific inflammation results from the stimulation of various pro-inflammatory mediators.

According to Senn *et al*.,[28] our study's analysis of the expression of these proinflammatory cytokines revealed that the diabetic control group had higher levels of these cytokines in their blood. They stated that type 2 diabetes and insulin resistance were linked to IL-6. The heart, liver, and pancreas all showed markedly lower cytokine levels after receiving Morin and metformin.

Cellular reactions to a variety of stimuli, including stress, cytokines, free radicals, UV light, and bacterial or viral antigens, are significantly influenced by NF-IB. NF-IB has been shown to play a proapoptotic role in numerous tests. Furthermore, in isolated peripheral blood mononuclear cells from individuals with type 1 diabetes, hyperglycemia causes NF-IB activation.[29] In mesangial cells, elevated glucose produces ROS, which causes NF-Ḅ to be upregulated. Similarly, oxidized LDL uses ROS to activate NF-B in mesangial and endothelial cells.

In the current study, the observed increase in NF-ƙB expression aligns with these previous studies. The diabetic control group exhibited increased NF-ƙB expression in heart, liver and pancreas which was reduced significantly when treated with Morin and metformin. The down-regulation of TNF-α, IL-6, and NF-Ḅ expression was similar for morin and metformin. Verma *et al*.,[30] demonstrated that morin can modulate the inflammatory pathways and attenuates the myocardial injury in diabetic rats.

The pancreas and liver of diabetic rats showed considerable tissue damage, according to histopathological examination. In diabetic rats, the morphological changes in the liver and pancreas were regulated by morin and metformin administration. In the liver, diabetic rats displayed hepatocyte degeneration, distorted portal veins, and parenchymal necrosis with evident inflammation, whereas normal rats showed healthy hepatocytes. Morin and metformin-treated diabetic rats exhibited near-normal liver morphology with mild hepatocyte degeneration. The pancreas of diabetic rats showed severe islet necrosis and atrophy, while normal rats had intact islet structures. Morin and metformin supplementation significantly reduced pancreatic necrosis and degeneration, restoring islet morphology to near-normal levels. These findings suggest that morin effectively mitigates diabetes-induced histopathological alterations, comparable to metformin.

Conclusion

In diabetic rats, morin significantly attenuated inflammatory markers (IL-6, TNF-α, and NF-κB) and improved the structural integrity of the liver and pancreas, demonstrating efficacy comparable to metformin. Both morin and metformin also contributed to better glycemic control, as evidenced by reduced blood glucose and HbA1c levels. These findings highlight morin's ability to counteract inflammation and tissue damage induced by diabetes. Further clinical research is essential to confirm its translational potential in human diabetes management.

Financial support and sponsorship

Nil.

Conflicts of interest

There are no conflicts of interest.

References

1. Drareni K, Gautier JF, Venteclef N, Alzaid F. Transcriptional control of macrophage polarisation in type 2 diabetes. Semin Immunopathol 2019;41:515-29.
2. Tanti JF, Grémeaux T, van Obberghen E, Le Marchand-Brustel Y. Serine/threonine phosphorylation of insulin receptor substrate 1 modulates insulin receptor signaling. J Biol Chem 1994;269:6051-7.
3. Tilg H, Moschen AR. Inflammatory mechanisms in the regulation of insulin resistance. Mol Med 2008;14:222-31.
4. Crook M. Type 2 diabetes mellitus: A disease of the innate immune system? An update. Diabet Med 2004;21:203-7.
5. Takeda K, Akira S. Toll-like receptors in innate immunity. Int Immunol 2005;17:1-14.
6. Luo P, Wang MH. Eicosanoids, β-cell function, and diabetes. Prostaglandins Other Lipid Mediat 2011;95:1-10.
7. Lekshmi RK, Rajesh R, Mini S. Ethyl acetate fraction of *Cissus quadrangularis* stem ameliorates hyperglycaemia-mediated oxidative stress and suppresses inflammatory response in nicotinamide/streptozotocin induced type 2 diabetic rats. Phytomedicine 2015;22:952-60.
8. Ansari P, Khan JT, Chowdhury S, Reberio AD, Kumar S, Seidel V, *et al*. Plant-based diets and phytochemicals in the management of diabetes mellitus and prevention of its complications: A review. Nutrients 2024;16:3709.
9. Jin H, Lee WS, Eun SY, Jung JH, Hyeon-Soo P, Kim G, *et al*. Morin, a flavonoid from *Moraceae*, suppresses growth and invasion of the highly metastatic breast cancer cell line MDA-MB231 partly through suppression of the Akt pathway. Int J Oncol 2014;45:1629-37.
10. Shyma RL, Mini S. Neuroprotective effect of Morin via TrkB/Akt pathway against diabetes mediated oxidative stress and apoptosis in neuronal cells. Toxicol Mech Methods 2022;32:695-704.
11. Huggett AS, Nixon DA. Use of glucose oxidase, peroxidase, and O-dianisidine in determination of blood and urinary glucose. Lancet 1957;273:368-70.
12. Trivelli LA, Ranney HM, Lai HT. Hemoglobin components in patients with diabetes mellitus. N Engl J Med 1971;284:353-7.
13. Shimizu T, Kondo K, Hayaishi O. Role of prostaglandin endoperoxides in the serum thiobarbituric acid reaction. Arch Biochem Biophys 1981;206:271-6.
14. Baccaglini PI, Hogan PG. Some rat sensory neurons in culture express characteristics of differentiated pain sensory cells. Proc Natl Acad Sci U S A 1983;80:594-8.
15. Salter M, Knowles RG. Assay of NOS activity by the measurement of conversion of oxyhemoglobin to methemoglobin by NO. Methods Mol Biol 1998;100:61-5.
16. Bradley PP, Priebat DA, Christensen RD, Rothstein G. Measurement of cutaneous inflammation: Estimation of neutrophil content with an enzyme marker. J Invest Dermatol 1982;78:206-9.
17. Lowry OH, Rosebrough NJ, Farr AL, Randall RJ. Protein measurement with the Folin phenol reagent. J Biol Chem 1951;193:265-75.
18. Chomczynski P, Mackey K. Short technical reports. Modification of the TRI reagent procedure for isolation of RNA from polysaccharide- and proteoglycan-rich sources. Biotechniques 1995;19:942-5.
19. Disbrey BD, Rack JH. Histological Laboratory Methods. Vol. 43. Edinburgh: Livingstone; 1970.
20. Bennet CA, Franklin NL. Statistical Analysis in Chemistry and the Chemical Industry. New York: John Wiley and Sons; 1967. p. 208-27.
21. Nagarchi K, Ahmed S, Sabus A, Saheb SH. Effect of streptozotocin on glucose levels in albino Wister rats. J Pharm Sci Res 2015;7:67-9.
22. Lin Y, Berg AH, Iyengar P, Lam TK, Giacca A, Combs TP, *et al*. The hyperglycemia-induced inflammatory response in adipocytes: The role of reactive oxygen species. J Biol Chem 2005;280:4617-26.
23. Mohammed HA, Al-Shamma GA, Hashim HM. Beta-carotene, glycemic control and dyslipidemia in type 2 diabetes mellitus. J Fac Med Baghdad 2006;48:4.
24. Shanmugam N, Gaw Gonzalo IT, Natarajan R. Molecular mechanisms of high glucose-induced cyclooxygenase-2 expression in monocytes. Diabetes 2004;53:795-802.
25. Pacher P, Obrosova IG, Mabley JG, Szabó C. Role of nitrosative stress and peroxynitrite in the pathogenesis of diabetic complications. Emerging new therapeutical strategies. Curr Med Chem 2005;12:267-75.
26. Olza J, Aguilera CM, Gil-Campos M, Leis R, Bueno G, Martínez-Jiménez MD, *et al*. Myeloperoxidase is an early biomarker of inflammation and cardiovascular risk in prepubertal obese children. Diabetes Care 2012;35:2373-6.
27. Akash MS, Rehman K, Chen S. Role of inflammatory mechanisms in pathogenesis of type 2 diabetes mellitus. J Cell Biochem 2013;114:525-31.
28. Senn JJ, Klover PJ, Nowak IA, Mooney RA. Interleukin-6 induces cellular insulin resistance in hepatocytes. Diabetes 2002;51:3391-9.
29. Hofmann MA, Schiekofer S, Kanitz M, Klevesath MS, Joswig M, Lee V, *et al*. Insufficient glycemic control increases nuclear factor-ƙB binding activity in peripheral blood mononuclear cells isolated from patients with type 1 diabetes. Diabetes Care 1998;21:1310-6.
30. Verma VK, Malik S, Mutneja E, Sahu AK, Prajapati V, Mishra P, *et al*. Morin ameliorates myocardial injury in diabetic rats via modulation of inflammatory pathways. Lab Anim Res 2024;40:3.

Original Article

Role of C-reactive Protein, D-dimer, and Ferritin in Predicting the Clinical Outcomes of COVID-19 Patients: A Retrospective Study

Julie Philipose Baby, Rennis Davis Kizhakkepeedika[1], Arun Narasingamoor Pillai[1], Aiwariya[2], Gini Muttath Paul[3], Vellappillil Raman Kutty[4]

Departments of Anaesthesiology, [1]Pulmonary Medicine, [2]Microbiology and [3]Biostatistics, Amala Instituite of Medical Sciences, [4]Amala Centre for Research Promotion, Thrissur, Kerala, India

Abstract

Background: A comprehensive understanding of the association between viral load, inflammatory markers on the day of admission, and disease outcomes in coronavirus disease-2019 (COVID-19) is significant for effective clinical management. The aim of this study was to know whether the initial viral load or inflammatory markers contributes to mortality and disease severity in COVID-19 patients. **Methods:** A retrospective study was designed among confirmed COVID-19 patients from August 2021 to May 2022. The patient demographics, cycle threshold (Ct) values, and inflammatory markers such as C-reactive protein (CRP), D-dimer, and ferritin levels were selected. The severity of the disease, as evidenced by the presence of respiratory failure requiring noninvasive or invasive mechanical ventilation and subsequent mortality as outcome, was meticulously examined. The data were statistically analyzed. **Results:** Receiver operating characteristic curve analysis revealed acceptable discriminatory capability between survival and mortality for D-dimer (AUC: 0.72), whereas CRP exhibited the highest discriminatory capacity (AUC: 0.85). The ferritin did not display significant discriminatory capacity (AUC: 0.61). A higher CT score was linked to less disease severity, while CRP demonstrated notable correlations with both disease severity and mortality. **Conclusion:** Viral load, as measured by CT values, along with CRP and D-dimer levels, were associated with the severity of COVID-19. Ferritin showed only a modest association with disease classification, whereas CRP alone predicted mortality. These findings offer critical insights for an early clinical management strategy to enhance patient outcomes.

Keywords: Coronavirus disease-2019, inflammatory markers, mortality, severity, viral load

Introduction

Upper respiratory tract (URT) infections are characterized by upper airway irritation and swelling that goes away on its own, along with a cough, but there is no evidence of pneumonia, no other illness that can explain the patient's symptoms, or no history of chronic bronchitis, emphysema, or chronic obstructive pulmonary disease.[1] The nose, sinuses, pharynx, larynx, and major airways are all affected by URT infections. Rhinoviruses, enteroviruses, adenoviruses, influenza viruses, respiratory syncytial viruses, coronaviruses, and parainfluenza viruses are the viruses most frequently linked to illnesses.[2-5] Infection with the severe acute respiratory syndrome coronavirus 2 (SARS CoV-2) virus has emerged as one of the major causes of hospitalizations and fatalities in nearly every region of the world in 2020. More research is required to determine whether the late inflammatory cascade or the early viral load contributes to virulence and major pathological outcomes. It is yet unknown how the severity of the coronavirus disease (COVID-19) is correlated with viral replication levels. Due to medical costs and lost productivity, viral respiratory tract infections have a significant negative economic impact on society.[6] Moreover, these individuals

Access this article online

Quick Response Code:

Website: https://journals.lww.com/hrcm/

DOI: 10.4103/JHCR.JHCR_4_25

Address for correspondence: Dr. Rennis Davis Kizhakkepeedika, Department of Pulmonary Medicine, Amala Institute of Medical Science, Thrissur, Kerala, India.
E-mail: dr.rennis@amalaims.org

Received: 22-03-2025 **Revised:** 28-04-2025
Accepted: 29-04-2025 **Published:** ***

How to cite this article: Baby JP, Kizhakkepeedika RD, Pillai AN, Aiwariya, Paul GM, Kutty VR. Role of C-reactive protein, D-dimer, and ferritin in predicting the clinical outcomes of COVID-19 patients: A retrospective study. J Adv Health Res Clin Med 2025;XX:XX-XX.

exhibited increased levels of inflammatory markers such as C-reactive protein (CRP) and interleukin-6 (IL-6), coupled with lower absolute lymphocyte counts. In contrast, an independent study by Argyropoulos *et al*. demonstrated that viral load did not exhibit a significant association with key clinical outcomes, including admission to the intensive care unit (ICU), requirement for oxygen support, and overall survival.[7] Several studies have presented conflicting evidence on the viral shedding and transmissibility of COVID-19, with no established link to clinical outcomes, as indicated by Liu *et al*.[8] The importance of identifying clinical parameters predicting disease outcomes was emphasized by Shlomai *et al*.[9] They suggested that viral load could serve as a rapid screening tool for assessing COVID-19 severity in admitted patients. In addition, Monson *et al*. proposed the identification of a high-risk inflammatory phenotype, COV-HI, for effective stratification of patient groups.[10] In a separate study, Magleby *et al*. found an independent correlation between SARS-CoV-2 viral load and the risk of intubation and mortality among hospitalized patients.[11]

Karahasan *et al*. examined the relationship between the overall severity score of radiological findings (CT) in COVID-19 participants and PCR Ct values.[12] Their findings underscored the importance of early viral load determination in preventing disease spread, with chest CT serving as a valuable tool for identifying cases requiring extensive medical care. Meanwhile, Ra *et al*. compared viral loads in asymptomatic and symptomatic individuals with infection.[13] They observed persistent positive upper respiratory reverse transcription polymerase chain reaction (RT-PCR) results in a substantial proportion of mildly symptomatic and asymptomatic individuals during follow-up, highlighting the potential for ongoing viral shedding in these groups despite lower viral loads.

Even though the asymptomatic COVID-19 patients had reduced viral levels, Zhou *et al*.'s investigation into their viral dynamics showed the potential for transmission and viral shedding.[14] It was acknowledged that further studies were warranted to precisely define the relationship between viral load, inflammatory markers, disease progression, and outcomes when these markers are analyzed on the day of admission. The aim of this study was to know whether the initial viral load (indirectly obtained by the CT value) or inflammatory markers contribute to mortality and disease severity.

Methods

Study designs and participants

This study was conducted retrospectively at our state's tertiary care center. Patients with confirmed COVID-19, during the time period of August 2021 to May 2022 through universal sampling. Samples obtained from patients with an average age of 57 ± 17 were included in the study. Only admitted patients diagnosed to be COVID-19 positive at our center were included. The patients who died within 24 h of admission, those without Ct and inflammatory marker values, and also those patients who discontinued treatment or transferred to different centers, or patients with chronic illness were excluded from the study. Ethics committee approval (No: 11/IEC/21/AIMS-21) and gatekeeper consent were obtained. The requirement for informed consent was waived by the ethics committee.

Study procedure

Each patient's electronic medical records were reviewed to determine demographics, clinical categorization of COVID 19, Ct values, blood levels of inflammatory markers such as C-reactive protein, D-dimer, ferritin, oxygenation status, complications during 1st day of admission, and outcome.

Detection of reverse transcription polymerase chain reaction

The sample was collected using a nasopharyngeal/throat swab as per standard institutional protocols. The confirmation of COVID-19 diagnosis relies on RT-PCR or confirmatory TRUENAT testing, wherein the viral load is indirectly assessed through the determination of Ct values. The viral load is stratified into three grades according to CT values: high viral load up to 24, moderate viral load 24–35, and mild viral load 35–40.

Analysis of inflammatory markers

The blood levels of inflammatory markers, such as serum CRP, plasma D-dimer, and serum ferritin, were assessed. For the evaluation of the CRP, samples collected in a clot activator without anticoagulant underwent centrifugation at 3000 rpm for 15 min to facilitate serum separation. CRP concentration in the serum of COVID-19 patients was quantified using the ELISA technique, adhering to the manufacturer's guidelines (Demeditec, Germany). For D-dimer test blood was drawn in a blue-topped tube containing sodium citrate. D-dimer analysis was conducted on a fully automated clinical chemistry analyzer (Abbott, Architect, USA). Circulating serum ferritin levels were measured using ELISA according to the manufacturer's guidelines (Pointe Scientific, Inc., USA). CRP levels were categorized as follows: 0–5.99 mg/dl considered normal, 6–25.99 mg/dl classified as mild, 26–100 mg/dl categorized as moderate, and >100 mg/dl deemed severe. D-dimer levels were interpreted as follows: <500 ng/ml considered normal, 500–1000 ng/ml indicative of mild elevation, and >1000 ng/ml indicating moderate-to-severe elevation, as supported by existing literature. The normal range for ferritin levels was defined as 13–150 ng/ml, with levels exceeding 150 ng/ml considered abnormal.

Determination of severity and outcome

Severity parameters encompass the duration of intensive care unit (ICU) stay, hospital stay, noninvasive mechanical ventilation (NIV), mechanical ventilation (MV) and outcome was analyzed from the mortality. Oxygenation status is determined by the need for oxygen support through various means such as nasal cannula, facemask, non-rebreathing mask, high-flow nasal oxygen (HFNO), noninvasive ventilation, or MV. Patients requiring oxygen therapy are categorized into two groups: the MV group, which includes intubated patients,

and the NIV group, which includes all other forms of oxygen therapy mentioned. Categorization of COVID-19 into Classes A, B, and C in accordance with State Guidelines Version 3 as of April 25, 2021.

Statistical analysis

Statistical analysis was done using SPSS 23 software. Mann-Whitney U test was used to compare the median values. Categorical variables are scrutinized in terms of frequencies and percentages and the association between variables was determined using Fisher's exact test, Logistic regression was done to find the odds ratio (OR) for the severity outcome of COVID-19. To evaluate the predictive value of D-dimer, CRP, and ferritin, for mortality, a receiver operating characteristic (ROC) analysis was done, and the area under the ROC curve (AUC), sensitivity, and specificity were calculated. $P < 0.05$ was considered significant.

Results

A total of 89 patients who tested positive for COVID-19 were included in the study. Gender-wise distribution of patients is given in Figure 1. Among them, 86.5% survived, 13.5% succumbed to the infection, and 56.2% were managed within the ward and subsequently discharged in stable condition. A further 4.5% necessitated ICU admission but were later discharged to the ward. Notably, 32.6% required NIV, while 6.7% necessitatedMV, resulting in fatality for all mechanically ventilated patients. The mean age of the study participants was 57 years, with a standard deviation of 17.0. Gender distribution revealed 53.9% of males and 46.1% of females.

Inflammatory markers and categorization

The analysis revealed no significant association between CT values and severity categories of COVID-19 illness. Our study findings indicated a significant correlation between CRP levels and the clinical categorization of COVID-19. In the analysis correlating CRP levels with categorized severity groups, a statistically significant correlation was observed ($P = 0.001$). The distribution of CRP levels across categories A, B, and C indicated a notable trend: as the severity of illness increased, CRP levels also increased.

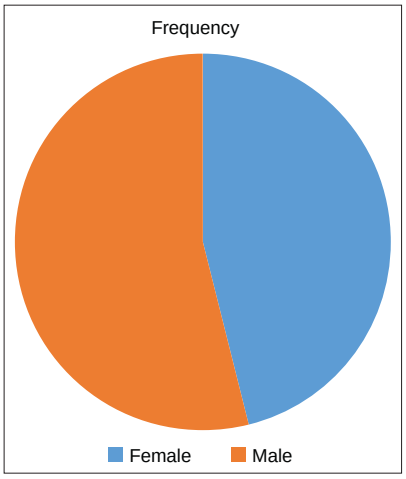

Figure 1: Gender wise distribution of patients

Moreover, no patients in category A had CRP levels between 6 and 25.99 mg/dl levels, 7 patients falling into category B, and 21 patients falling into category C within this CRP range. Similarly, no patients in category A had CRP levels between 26 and 100 mg/dl, with 1 and 8 patients, respectively, in categories B and C falling within this range. Furthermore, only one patient in category C had CRP levels exceeding 100 mg/dl. This suggested a significant association between CRP levels and the category of COVID-19 illness [Table 1].

No statistically significant correlation was found between D-dimer levels and the categorized groups of COVID-19 patients ($P = 0.155$). The analysis revealed a statistically significant association between serum ferritin levels and categorical groups (A, B, and C) ($P = 0.048$). Specifically, among individuals with ferritin levels <150 ng/ml, there were 3, 7, and 8 in categories A, B, and C, respectively. Conversely, for those with ferritin levels exceeding 150 ng/ml, there were 1, 15, and 36 in categories A, B, and C, respectively. This suggests that higher serum ferritin levels may correlate with an increased chance of being in category C compared to others [Table 1].

Disease severity, computed tomography value, and inflammatory markers

In our study, there is a statistically significant association between CT values and oxygen requirement among patients

Table 1: Correlation between categorization and inflammatory markers

	Category			Total	*P* (Fisher's exact test)
	A (%)	B (%)	C (%)		
CRP (mg/dL)					
<6	5 (100)	17 (68)	10 (25)	32	0.001
6–25.99	0	7 (28)	21 (52.5)	28	
26–100	0	1 (4)	8 (20)	9	
>100	0	0	1 (2.5)	1	
Total	5	25	40	70	
Ferritin					
<150	3 (75)	7 (3.1)	8 (1.81)	18	0.048
>150	1 (25)	15 (68.18)	36 (81.81)	52	
Total	4	22	44	70	
D-dimer					
<500	4 (57.1)	5 (14.7)	4 (8.5)	13	0.155
500–1000	1 (14.28)	8 (23.52)	9 (18.75)	18	
1001–3000	1 (14.28)	12 (35.29)	18 (37.5)	31	
>3000	1 (14.28)	9 (26.47)	17 (35.41)	27	
Total	7	34	48	89	
CT value					
>35	0	1 (2.9)	5 (10.6)	6	0.179
24–35	6 (85.7)	18 (52.9)	29 (61.7)	53	
<24	1 (14.28)	15 (44.11)	13 (27.65)	29	
Total	7	34	47	88	

P<0.05 are considered significant. CRP: C reactive protein, CT: Cycle threshold

with COVID-19. As CT values decrease (The lowest Ct value observed was 11), there is a notable increase in the need for oxygen support. This relationship is supported by a significant $P = 0.018$, suggesting that the need of requiring oxygen therapy rises as CT values decline [Table 2].

Among the patients with CRP levels <6 ng/ml, none required ICU admission or MV, with 100% (26 out of 26) managed in the ward, and 23.1% (6 out of 26) receiving NIV. As CRP levels increased, there was a notable escalation in acuity, with 30% (3 out of 10) of patients in the ward and 70% (7 out of 10) in the ICU with CRP levels ranging from 6 mg/dl to 25.99 mg/dl, and 100% (1 out of 1) in the ward with CRP levels between 26 and 100 mg/dl requiring NIV. Notably, among patients with CRP levels between 6 and 25.99 mg/dl, 15.4% (2 out of 13) required MV. In addition, among those with CRP levels exceeding 100 mg/dl, none were admitted to the ward, with one patient requiring NIV. The $P = 0.0001$ underscores a significant association between CRP levels and the need for oxygen support.

There is a statistically significant association between D-dimer levels and the severity of COVID-19 illness, as indicated by the need for oxygen support. As D-dimer levels increase, there is a significant escalation in the requirement for oxygen therapy. This association is underscored by a $P = 0.005$, suggesting a strong association between higher D-dimer levels and the likelihood of requiring oxygen support, ranging from noninvasive to mechanical ventilation. There is no significant association between serum ferritin levels disease severity among the studied population.

Mortality and disease severity with inflammatory markers

Table 3 shows that a more significant association was observed between CRP levels and mortality ($P = 0.001$), particularly evident in patients with CRP >100, where a higher death rate was observed, while CT value and ferritin exhibited no association with mortality. Among the 32 patients with CRP levels <6 mg/dL, 31 survived, while 1 died. In the group of 28 patients with CRP levels ranging from 6 to 25.99 mg/dL, 24 patients survived and 4 died. Among 9 patients with CRP levels between 26 and 100 mg/dL, 4 patients survived, and 5 died. Among 70 patients with CRP levels exceeding 100 mg/dL, 59 survived, and 11 died. In this study, 12 patients died with D-dimer >1000 ng/ml ($P = 0.017$).

Overall, out of the 89 patients analyzed, 77 survived (86.5% survival rate), and 12 died (13.5% mortality rate). Higher D-dimer levels associated with increased mortality rates. It is noteworthy to mention that out of the eight deaths observed in patients with D-dimer levels were above 3000 ng/mL. Median value of D-dimer and CR*P* values were seen high in dead patients, of these, CRP levels are seen high with a significant $P = 0.0001$ [Table 4].

In the case of multivariate logistic regression model, all these inflammatory markers and CT value showed to be a risk factor for mortality with an odds ratio(>1). In the analysis, D-dimer, ferritin, and CT were found to show a risk trend, suggesting a potential association with the outcome variable. However, it is noteworthy that this association did not reach statistical significance [Table 5]. Therefore, while there may be a trend

Table 2: Association between disease severity, cycle threshold value and inflammatory markers

	Coding for severity in survived/died				Total	*P* (Fisher's exact test)
	Ward stay (%)	ICU (%)	NMV (%)	MV (%)		
CT value						
>35	0	0	6 (21.4)	0	6	0.018
24–35	33 (66)	3 (75)	13 (46.4)	4 (66.6)	53	
<24	17 (34)	1 (25)	9 (32.14)	2 (33.3)	29	
Total	50	4	28	6	88	
CRP (mg/dL)						
<6	26 (70)	0	6 (24)	0	32	0.0001
6–25.99	10 (27)	3 (100)	13 (52)	2 (40)	28	
26–100	1 (2.7)	0	5 (20)	3 (60)	9	
>100	0	0	1 (4)	0	1	
Total	37	3	25	5	70	
D-dimer (ng/mL)						
<500	10 (20)	0	3 (10.3)	0	13	0.005
500–1000	14 (28)	0	4 (13.79)	0	18	
1001–3000	18 (36)	0	11 (37.9)	2 (33.3)	31	
>3000	8 (16)	4 (100)	11 (37.9)	4 (66.6)	27	
Total	50	4	29	6	89	
Ferritin (ng/mL)						
<150	12 (33.3)	0	3 (12)	3 (50)	18	0.063
>150	24 (66.6)	3 (100)	22 (88)	3 (50)	52	
Total	36	3	25	6	70	

P<0.05 are considered significant. CRP: C reactive protein, ICU: Intensive care unit, NMV: Noninvasive MV, MV: Mechanical ventilation, Ct: Cycle threshold

Table 3: Mortality and disease severity

	Out come		Total	*P* (Fisher's exact test)
	Survived (%)	Death (%)		
CRP (mg/dL)				
<6	31 (52)	1 (9)	32	0.001
6–25.99	24 (40.67)	4 (36)	28	
26–100	4 (6)	5 (45)	9	
>100	0	1 (9)	1	
Total	59	11	70	
D-dimer (ng/mL)				
<500	13 (16.8)	0	13	0.017
500–1000	17 (22)	1 (8)	18	
1001–3000	28 (36.3)	3 (25)	31	
>3000	19 (24.6)	8 (66.6)	27	
Total	77 (86.5)	12 (13.5)	89	
Ferritin (ng/mL)				
<150	15 (25.8)	3 (25)	18	0.950
>150	43 (74.13)	9 (75)	52	
Total	58	12	70	

P<0.05 are considered significant, CRP: C reactive protein

Table 4: Ferritin, C-reactive protein, and D-dimer levels in the blood of patients who deceased and survived

Markers	Death	Survived	*P*
D-dimer (ng/mL)	4136 (8123)	1361 (1949)	0.001
CRP (mg/dL)	40.6 (68.6)	6.5 (12.2)	0.0001
Ferritin (ng/mL)	1049 (1075)	378.3 (755.2)	0.114

Data expressed as median (IQR). *P* value (Mann–Whitney *U*-test) *P*<0.05 are considered significant. D-dimer (*n*=89), CRP (*n*=70), Ferritin (*n*=70). CRP: C reactive protein, IQR: Interquartile range

Table 5: Multiple logistic regression model of the study variables

Marker	*P*	OR	95% CI	
			Lower	Upper
D-dimer	0.117	1.000	1.000	1.000
CRP	0.047	1.045	1.001	1.092
Ferritin	0.791	1.000	1.000	1.001
CT	0.755	1.022	0.891	1.173
Age	0.050	1.099	1.000	1.209

CRP: C reactive protein, CT: Cycle threshold, CI: Confidence interval, OR: Odds ratio

indicating these variables as potential risk factors, the results did not demonstrate a conclusive statistical relationship between D-dimer, ferritin, CT, and mortality in this study.

Age and CRP, however, indicate a significant risk of death ($P < 0.05$) [Table 5].

The ROC curve analysis [Figure 2] revealed acceptable discriminatory capability between survival and mortality for D-dimer (Area under the curve: 0.72, standard error: 0.07; 95% confidence interval [CI]: 0.57-0.88, $P = 0.007$). A cut-off value of ≥1000 ng/ml for D-dimer demonstrated a sensitivity of 0.92 and a specificity of 0.39. Similarly, CRP exhibited the highest discriminatory capacity between mortality and survival (area under the curve: 0.85, standard error: 0.06; 95% CI: 0.73–0.97, $P = 0.001$). Using a cutoff value of ≥26.00 mg/dl for CRP yielded a sensitivity of 0.55 and a specificity of 0.93 for mortality prediction. On the contrary, the ROC curve for ferritin did not display significant discriminatory capacity (area under the curve: 0.61, standard error: 0.08; 95% CI: 0.45–0.77, $P = 0.19$).

Discussion

The COVID-19 pandemic has emerged as one of the most defining events of the 21st century, causing widespread fear and uncertainty.[15] Biomarkers of inflammation indicative of hyperinflammatory states and disease severity in COVID-19 patients were reported in previous studies.[16-18] Zhou *et al*. observed that elevated D-dimer levels (≥1000 ng/mL) on admission among COVID-19 patients corresponded to a higher mortality rate.[18] Similarly, according to Fajnzylber *et al*., there may be a connection between viral load, inflammatory response, and disease severity because patients with higher viral loads typically have lower absolute lymphocyte counts but higher levels of CRP, IL-6, lactate dehydrogenase, D-dimer, and other inflammatory markers.[19]

COVID-19 has also been linked to fibrinolysis, coagulation activation, and pulmonary microvascular immune thrombosis through the immune-thrombotic pathway. Increased D-dimer supports the elevated production of thrombin and, thus, risk for thrombosis.

An indication of this process, D-dimer, has been linked to the disease as a prognostic predictor.[20] This study validates the predictive significance of D-dimer levels, using elevated levels at admission as a reliable predictor of in-hospital mortality and correlated with the severity of the disease, which is in consistent with the previous study by Yao *et al*.[21] Notably, a cutoff value of ≥1000 ng/ml for D-dimer in our results demonstrated a sensitivity of 92 and a specificity of 39 in predicting mortality. However, the OR was not significant to support this as a predictor of mortality. This may probably be due to the small sample size of the study.

Although earlier studies have demonstrated the predictive importance of CRP and D-dimer, our investigation goes one step further by assessing ferritin levels as well. Although ferritin levels exhibited some correlation with the categorization of COVID-19 patients, they did not demonstrate significant associations with disease severity or mortality. Hence, it is not a widely acknowledged or trustworthy predictor, and its contribution may be less significant than that of other markers such as CRP or D-dimer. While CRP and D-dimer may serve as valuable markers for assessing disease severity and predicting mortality.

The Ct count, as determined by RT-PCR, is inversely proportional to viral load, which in turn can help determine

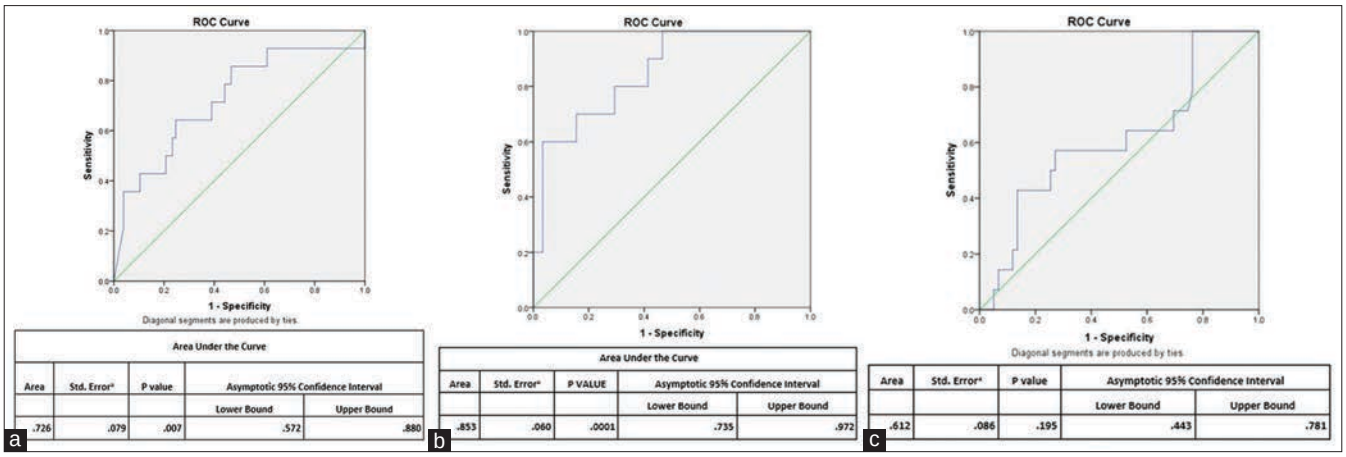

Figure 2: Receiver operating characteristic curve of the inflammatory markers. (a) D-dimer, (b) C-reactive protein and (c) Ferritin

clinical progress and outcome.[22] In our study, we aimed to investigate the impact of viral load (CT values) on the severity of COVID-19 disease and the influential factor for predicting disease progression. A significant correlation between CT values and disease severity was found in our study, suggesting that more severe sickness was associated with larger viral loads. A previous study found that there was no statistically significant difference in the severity of COVID-19 between Ct values.[23]

The role of ferritin and iron metabolism in COVID-19 infection remains a subject of debate. Several studies have reported elevated levels of ferritin in patients with severe COVID-19 infections compared to other infections, suggesting a potential association with disease severity. However, ferritin is not yet considered a standard predictive inflammatory marker in COVID-19 infection.[24] Qin *et al*. observed an increase in ferritin levels in a significant proportion of COVID-19 patients, and the elevation was suggested to be linked with poor clinical outcomes.[25] Nevertheless, of these results, this study found that ferritin levels in COVID-19 patients did not significantly correlate with illness severity or mortality. John *et al*. found that elevated levels of polymorphs, LDH, ferritin, D-dimer, and high sensitivity-CRP in COVID-19 patients with low E gene Ct values were associated with increased disease severity and mortality. This shows that low E gene Ct levels may act as an early warning sign for patients at risk of serious outcomes.[26] Acute-phase protein CRP, which is generated by the liver and triggered by a number of inflammatory mediators, including IL-6, has been thoroughly investigated as a biomarker for infection and inflammation.[27] CRP is a marker for inflammation, which is usually increased in patients with COVID-19, diabetes mellitus, depression, smoking, obesity, and even in sleep deprivation. Yang *et al*. examined 85 COVID-19 patients, and 96.47% of them had elevated CRP levels, which are correlated with the severity of the illness.[28] For mortality prediction, our study's threshold value of ≥ 26.00 mg/dl for CRP produced a sensitivity of 0.55 and a specificity of 0.93. The robust association of CRP with these outcomes underscores its potential utility as a prognostic marker in COVID-19 management. However, the results should be interpreted cautiously in people with other comorbidities, which can alter CRP levels. The elevated significant value of ferritin and CRP can be explained by the comorbidities associated with those patients. In multiple logistic regression analysis, age emerged as a confounding factor ($P = 0.05$) in mortality prediction.

Higher mortality and severity of disease were linked to high CR*P* values, a sign that may be evaluated both at presentation and during categorization. Such patients should be managed with stringent measures. To reduce mortality, patients with high D-dimer levels must be carefully managed with anticoagulants. Our study found that individuals with low Ct values had severe illness and typically had poor performance.

The limitations of this study include a very small sample size, which implies that these findings should be validated in larger populations. The lack of patient data is the cause of the difference in the number of samples in the inflammatory markers. Moreover, as this was a single-center study, the analysis focused solely on inflammatory markers such as CRP, D-dimer, and ferritin, potentially limiting the comprehensiveness of our findings. In addition, the comorbidities of patients in categories A, B, and C were not taken into consideration.

Conclusion

The CT values were significantly associated with the severity of COVID-19 illness. Among inflammatory markers, CRP demonstrated a significant association with categorization, severity, and mortality. D-dimer demonstrated a strong relationship with severity but no association with categorization or predicting mortality. The study thus highlights the importance of measuring CRP and D-dimer on the day of admission.

Acknowledgment

The authors would like to express their gratitude for the valuable support provided by Dr. AT Francis, Professor and

Head of The Department and Dr. Binitha PP, Research Officer Department of Library and Research Documentation, Amala Institute of Medical Sciences, Amala Nagar, Thrissur.

Financial support and sponsorship

Nil.

Conflicts of interest

There are no conflicts of interest.

References

1. Wenzel RP, Fowler AA 3rd. Clinical practice. Acute bronchitis. N Engl J Med 2006;355:2125-30.
2. Denny FW Jr. The clinical impact of human respiratory virus infections. Am J Respir Crit Care Med 1995;152:S4-12.
3. Pavia AT. Viral infections of the lower respiratory tract: Old viruses, new viruses, and the role of diagnosis. Clin Infect Dis 2011;52 Suppl 4:S284-9.
4. Drieghe S, Ryckaert I, Beuselinck K, Lagrou K, Padalko E. Epidemiology of respiratory viruses in bronchoalveolar lavage samples in a tertiary hospital. J Clin Virol 2014;59:208-11.
5. Esposito S, Daleno C, Prunotto G, Scala A, Tagliabue C, Borzani I, *et al.* Impact of viral infections in children with community-acquired pneumonia: Results of a study of 17 respiratory viruses. Influenza Other Respir Viruses 2013;7:18-26.
6. Kotwani A, Holloway K. Antibiotic prescribing practice for acute, uncomplicated respiratory tract infections in primary care settings in New Delhi, India. Trop Med Int Health 2014;19:761-8.
7. Argyropoulos KV, Serrano A, Hu J, Black M, Feng X, Shen G, *et al.* Association of initial viral load in severe acute respiratory syndrome coronavirus 2 (SARS-CoV-2) patients with outcome and symptoms. Am J Pathol 2020;190:1881-7.
8. Liu Y, Yan LM, Wan L, Xiang TX, Le A, Liu JM, *et al.* Viral dynamics in mild and severe cases of COVID-19. Lancet Infect Dis 2020;20:656-7.
9. Shlomai A, Ben-Zvi H, Glusman Bendersky A, Shafran N, Goldberg E, Sklan EH. Nasopharyngeal viral load predicts hypoxemia and disease outcome in admitted COVID-19 patients. Crit Care 2020;24:539.
10. Manson JJ, Crooks C, Naja M, Ledlie A, Goulden B, Liddle T, *et al.* COVID-19-associated hyperinflammation and escalation of patient care: A retrospective longitudinal cohort study. Lancet Rheumatol 2020;2:e594-602.
11. Magleby R, Westblade LF, Trzebucki A, Simon MS, Rajan M, Park J, *et al.* Impact of severe acute respiratory syndrome coronavirus 2 viral load on risk of intubation and mortality among hospitalized patients with coronavirus disease 2019. Clin Infect Dis 2021;73:e4197-205.
12. Karahasan Yagci A, Sarinoglu RC, Bilgin H, Yanılmaz Ö, Sayın E, Deniz G, *et al.* Relationship of the cycle threshold values of SARS-CoV-2 polymerase chain reaction and total severity score of computerized tomography in patients with COVID 19. Int J Infect Dis 2020;101:160-6.
13. Ra SH, Lim JS, Kim GU, Kim MJ, Jung J, Kim SH. Upper respiratory viral load in asymptomatic individuals and mildly symptomatic patients with SARS-CoV-2 infection. Thorax 2021;76:61-3.
14. Zhou R, Li F, Chen F, Liu H, Zheng J, Lei C, *et al.* Viral dynamics in asymptomatic patients with COVID-19. Int J Infect Dis 2020;96:288-90.
15. Sadati AK, Lankarani MH, Lankarani KB. Risk society, global vulnerability and fragile resilience; Sociological view on the coronavirus outbreak. Shiraz E Med J 2020;21:e102263.
16. Chen L, Liu HG, Liu W, Liu J, Liu K, Shang J, *et al.* Analysis of clinical features of 29 patients with 2019 novel coronavirus pneumonia. Chin J Tuberc Respir Dis 2020;43:E005.
17. Berenguer J, Ryan P, Rodríguez-Baño J, Jarrín I, Carratalà J, Pachón J, *et al.* Characteristics and predictors of death among 4035 consecutively hospitalized patients with COVID-19 in Spain. Clin Microbiol Infect 2020;26:1525-36.
18. Zhou F, Yu T, Du R, Fan G, Liu Y, Liu Z, *et al.* Clinical course and risk factors for mortality of adult inpatients with COVID-19 in Wuhan, China: A retrospective cohort study. Lancet 2020;395:1054-62.
19. Fajnzylber J, Regan J, Coxen K, Corry H, Wong C, Rosenthal A, *et al.* SARS-CoV-2 viral load is associated with increased disease severity and mortality. Nat Commun 2020;11:5493.
20. Townsend L, Fogarty H, Dyer A, Martin-Loeches I, Bannan C, Nadarajan P, *et al.* Prolonged elevation of D-dimer levels in convalescent COVID-19 patients is independent of the acute phase response. J Thromb Haemost 2021;19:1064-70.
21. Yao Y, Cao J, Wang Q, Shi Q, Liu K, Luo Z, *et al.* D-dimer as a biomarker for disease severity and mortality in COVID-19 patients: A case control study. J Intensive Care 2020;8:49.
22. Kim C, Kim JY, Lee EJ, Kang YM, Song KH, Kim ES, *et al.* Clinical findings, viral load, and outcomes of COVID-19: Comparison of patients with negative and positive initial chest computed tomography. PLoS One 2022;17:e0264711.
23. Atique M, Ghafoor A, Javed R, Fatima N, Yousaf A, Zahra S. Correlation of viral load with the clinical and biochemical profiles of COVID-19 patients. Cureus 2021;13:e16655.
24. Banchini F, Cattaneo GM, Capelli P. Serum ferritin levels in inflammation: A retrospective comparative analysis between COVID-19 and emergency surgical non-COVID-19 patients. World J Emerg Surg 2021;16:9.
25. Qin Z, Zhang X, Chen Z, Liu N. Establishment and validation of an immune-based prognostic score model in glioblastoma. Int Immunopharmacol 2020;85:106636.
26. John JE, Amle DB, Takhelmayum R, Gopal N, Mishra M, Joshi P, *et al.* Association of COVID-19 real-time reverse transcription-polymerase chain reaction (RT-PCR) cycle threshold value with surrogate markers of disease severity. Cureus 2022;14:e31034.
27. Valkanova V, Ebmeier KP, Allan CL. CRP, IL-6 and depression: A systematic review and meta-analysis of longitudinal studies. J Affect Disord 2013;150:736-44.
28. Yang W, Cao Q, Qin L, Wang X, Cheng Z, Pan A, *et al.* Clinical characteristics and imaging manifestations of the 2019 novel coronavirus disease (COVID-19): A multi-center study in Wenzhou city, Zhejiang, China. J Infect 2020;80:388-93.

Case Report

Role for Partial Peroneus Longus Tendon Graft and Adipofascial Lateral Supramalleolar Flap in Reconstruction of Posttraumatic Dorsal Foot Defect

Pradeoth Mukundan Korambayil, Avani K. Sunil, Avelyn Thazhuthadath Kishore

Department of Plastic Surgery and Burns, Jubilee Mission Medical College and Research Institute, Thrissur, Kerala, India

Abstract

Dorsal foot defects can be difficult to reconstruct, particularly when there is substantial soft-tissue damage and loss of toe extensor tendons. This case study presents the use of a partial peroneus longus tendon graft and an adipofascial lateral supramalleolar flap to reconstruct a posttraumatic dorsal foot defect. A 25-year-old male suffered a crush injury to his right foot, exposing the damaged toe extensor tendons. The partial peroneus longus tendon graft provided a structural foundation for segmental tendon reconstruction of the defect, while the reversed adipofascial lateral supramalleolar flap offered adequate soft-tissue coverage. The patient achieved adequate functional and cosmetic results postsurgery, without complications. This case study highlights the potential of utilizing a partial peroneus longus tendon graft instead of tensor fascia lata for tendon reconstruction and an adipofascial flap for complex dorsal foot defects, thereby reducing the morbidity associated with other extensive procedures typically required for crush injuries of the dorsum of the foot.

Keywords: Adipofascial lateral supramalleolar flap, dorsal foot defects, partial tendon graft, tendon reconstruction

Introduction

Dorsal foot soft-tissue defects can occur due to various causes, including trauma (such as accidents or injuries), infections, or underlying medical conditions. They can range from minor abrasions to severe wounds that may involve loss of skin, tendon, muscle, or bone. Treatment for dorsal foot soft-tissue defects often involves wound debridement and surgical reconstruction to restore function and appearance. Numerous techniques ranging from skin grafting to free tissue transfer have been utilized to reconstruct soft-tissue defects in the sole and proximal foot regions.[1] A dependable, straightforward, and secure reconstructive option is necessary for reconstructing the foot region. The lateral supramalleolar flap is raised on the lateral side of the lower leg and is vascularized by a perforating branch of the dorsal peroneal artery.[2,3] The lateral supramalleolar flap is frequently used for coverage encompassing the entire dorsum of the foot, the medial and lateral arches, and all areas of the heel region.[2,3] Modification of the lateral supramalleolar flap to adipofascial fashion increases the versatility of the flap for dorsal foot reconstruction.[4] Extensor tendon reconstruction was done with a partial tendon graft from the peroneus longus tendon.[5] This case report demonstrates the effectiveness of using a partial peroneus longus tendon graft and adipofascial flap from the leg for reconstructing complex dorsal foot defects. This approach minimizes the potential harm to the leg compared to other areas that might be required for dorsal foot reconstructions.

Access this article online

Quick Response Code:

Website: https://journals.lww.com/hrcm/

DOI: 10.4103/JHCR.JHCR_21_24

Case Report

A 25-year-old male, with no known comorbidities, sustained crush injury to the dorsum of his right foot in a road traffic accident, which was treated elsewhere and presented to the

Address for correspondence: Dr. Pradeoth Mukundan Korambayil, Department of Plastic Surgery and Burns, Jubilee Mission Medical College and Research Institute, Thrissur - 680 005, Kerala, India.
E-mail: pradeoth@gmail.com

Received: 26-09-2024 **Revised:** 04-04-2025
Accepted: 05-04-2025 **Published:** ***

How to cite this article: Korambayil PM, Sunil AK, Kishore AT. Role for partial peroneus longus tendon graft and adipofascial lateral supramalleolar flap in reconstruction of posttraumatic dorsal foot defect. J Adv Health Res Clin Med 2025;XX:XX-XX.

plastic surgery department on day 6 postinjury. On physical examination, there was a 10 cm × 5 cm × 2 cm soft-tissue loss on the dorsum of the foot with exposed tendons and restricted extension of lateral four toes with sutured laceration in the midleg region [Figure 1]. Furthermore, soft-tissue loss of 3 cm × 2 cm × 1 cm on the medial and plantar aspect of all toes was noted. Surgery was done under the femoral block. Intraoperatively, wound exploration revealed completely cut extensor tendons of 2nd, 3rd, 4th, and 5th toes [Figure 2]. Wound debridement, exploration, and tendon repair were performed. Soft-tissue repositioning was done to cover the exposed tendons; the wound was closed in layers [Figure 3a]. Vacuum-assisted closure (VAC) dressing was applied. The patient was immobilized on a below-knee plaster of paris (POP) slab in a neutral position of the right foot for 6 weeks. On removal of VAC dressing after 7 days, segmental necrosis of the extensor tendon of the 2nd and 3rd toes was seen. Furthermore, soft-tissue defect over the ankle region with exposed repaired tendon was noted.

The patient was posted for surgery under general anesthesia for wound debridement and exploration was done. Tendon reconstruction was done with a partial tendon graft from the peroneus longus tendon. Lateral supramalleolar flap cover of adipofascial type was performed [Figure 3b]. A flap inset was done following the reconstruction of the tendon. The donor area was closed by primary suturing. Graft was harvested from the right thigh and skin grafting was done over the adipofascial flap [Figure 3c]. The wound was closed in layers and dressing was applied. The patient was immobilized on a below-knee POP slab in a neutral position of the right foot for 6 weeks. Postoperative period was uneventful and was managed with intravenous antibiotics and analgesics. The patient was then discharged on postoperative day 9 and followed up at the outpatient clinic. In the follow-up period, the wound healed well with a healthy flap and graft covering the soft-tissue defect [Figure 3d]. During the follow-up period, the extension of the toe was adequate.

Discussion

Various techniques have been documented for reconstructing soft-tissue defects in the distal third of the leg, ankle, and foot region. Commonly employed procedures for resurfacing these defects include skin grafts, local pedicled flaps, distally and proximally based island flaps, cross-leg flaps, and free skin and muscle flaps. Distally based fasciocutaneous flaps on the leg and foot were introduced in 1983.[6] The primary advantages of these distally based flaps are a well-defined surface that is not dependent on a length–width ratio and the preservation of the main vascular axis. Two types of distally based pedicle flaps are frequently used to reconstruct soft-tissue defects in the foot region: the reverse sural artery flap and the lateral supramalleolar flap.[2,3] These flaps can be harvested as fasciocutaneous, islanded fasciocutaneous, adipofascial, propeller, or extended flaps, potentially incorporating flap delay procedures.

Venous congestion is a common complication in distally based flaps from the lower extremity. This is often due to factors such as compression of the flap's pedicle, valvular dysfunction, edema, compartment syndrome, or hematoma. Zayed reported venous congestion in 5 out of 25 lateral supramalleolar flaps, with varying degrees of severity.[7] Voche *et al*. observed venous congestion and partial flap necrosis in 41 cases using the lateral supramalleolar flap for ankle and foot defects.[3] A notable advantage of the adipofascial harvest of this flap is its thinness and reduced donor-site morbidity. In addition, the main arteries of the limb remain preserved during the dissection of the lateral supramalleolar flap.[2] Identifying the peroneus longus tendon is easier when the lateral supramalleolar flap is elevated along with the lateral septum. After the harvest of the partial tendon, tenodesis of the peroneus longus and peroneus brevis tendons can be performed to prevent reduced eversion and ankle instability.[8]

Conclusion

This case report presents a successful reconstruction of a complex dorsal foot defect using a partial peroneus longus tendon graft and an adipofascial lateral supramalleolar flap. The combination of these two techniques provided a robust and durable solution for the patient, resulting in adequate functional and esthetic outcomes. The use of a partial peroneus longus tendon graft offers several advantages, including reduced donor-site morbidity compared to other tendon grafts. In addition, the adipofascial lateral supramalleolar flap

Figure 1: Dorsal foot defect with gross contamination on day 6 following injury

Figure 2: Dorsal foot defect after debridement and exploration exposing the crushed tendon

Figure 3: (a) Stage 1: Reconstruction using local tissue mobilization and covering the tendon; (b) Stage 2: Reconstruction done for reconstruction of segmental tendon loss with partial peroneus longus and adipofascial lateral supramalleolar flap cover; (c) Skin graft applied over the adipofascial flap and donor area closed primarily; and (d) Late postoperative picture of healed wound and soft-tissue cover

provides reliable soft-tissue coverage with minimal donor-site complications.

Declaration of patient consent

The authors certify that they have obtained all appropriate patient consent forms. In the form, the patient has given his consent for his images and other clinical information to be reported in the journal. The patient understands that his name and initials will not be published and due efforts will be made to conceal his identity, but anonymity cannot be guaranteed.

Financial support and sponsorship

Nil.

Conflicts of interest

There are no conflicts of interest.

References

1. Sommerlad BC, McGrouther DA. Resurfacing the sole: Long-term follow-up and comparison of techniques. Br J Plast Surg 1978;31:107-16.
2. Demiri E, Foroglou P, Dionyssiou D, Antoniou A, Kakas P, Pavlidis L, *et al.* Our experience with the lateral supramalleolar island flap for reconstruction of the distal leg and foot: A review of 20 cases. Scand J Plast Reconstr Surg Hand Surg 2006;40:106-10.
3. Voche P, Merle M, Stussi JD. The lateral supramalleolar flap: Experience with 41 flaps. Ann Plast Surg 2005;54:49-54.
4. Kwon BK, Chung DW, Lee JH, Choi IH, Song JH, Lee SW. One-stage reverse lateral supramalleolar adipofascial flap for soft tissue reconstruction of the foot and ankle joint. J Korean Microsurg Soc 2007. p. 93-9.
5. Zhao J, Huangfu X. The biomechanical and clinical application of using the anterior half of the peroneus longus tendon as an autograft source. Am J Sports Med 2012;40:662-71.
6. Donski P, Fogdestam I. Distally based fasciocutaneous flap from the Sural region. A preliminary report. Plastic Reconstr Surg 1985;75:779.
7. Zayed EF. Lateral supramalleolar flap for reconstruction of the distal leg and foot, clinical experience with 25 cases. Methods 2011;12:17.
8. Budhiparama NC, Rhatomy S, Phatama KY, Chandra W, Santoso A, Lumban-Gaol I. Peroneus longus tendon autograft: A promising graft for ACL reconstruction. Video J Sports Med 2021;1:26350254211009888.

Case Report

Superficial Siderosis of the Central Nervous System Secondary to Spinal Myxopapillary

D. I. Devikrishna, Jijo Joseph, Robert P. Ambooken, Scott C. John[1]

Departments of Radiodiagnosis and [1]Orthopedics, Amala Institute of Medical Sciences, Thrissur, Kerala, India

Abstract

Superficial siderosis (SS) involving the brain and spinal cord is a rare and slowly progressive disease secondary to the deposition of hemosiderin within the meninges of the central nervous system. Identifying the primary cause of SS is essential for further management. We discuss here, the case of a 32-year-old male who was diagnosed as spinal myxopapillary ependymoma on contrast-enhanced magnetic resonance imaging (MRI) of the spine, which was later confirmed by excision biopsy. MRI brain was done for metastatic workup which showed features of SS. Myxopapillary ependymoma was concluded as the cause of SS by retrospective correlation and was managed accordingly.

Keywords: Angiography, ependymoma, siderosis

Introduction

Superficial siderosis (SS) affecting the brain and spinal cord is a rare and chronic disorder occurring due to the deposition of chronic blood products in the subpial layers secondary to chronic subarachnoid hemorrhage.[1] A patient with SS is usually asymptomatic but the classic presentations include adult-onset gait ataxia, cerebellar dysarthria, and sensorineural hearing impairment.[2] The development of symptoms attributable to SS usually occurs many decades after the inciting event. Magnetic resonance imaging (MRI) brain is considered the imaging modality of choice for the diagnosis of SS. The closest differential for SS is acute subarachnoid hemorrhage which is a medical emergency and hence it is ideal for radiologists to know about SS and how to differentiate them. Here, we discuss the case of a 32-year-old biopsy-proven case of myxopapillary ependymoma with SS.

Case Report

A 32-year-old male presented with complaints of chronic low back pain for 3 months. No past history of trauma is present. No obvious focal neurological deficits, focal tenderness, or deformities were detected on clinical examination. He was evaluated for back pain using contrast-enhanced MRI of the lumbar spine. The MRI depicted the presence of a T1 hypointense, T2, and short tau inversion recovery hyperintense, expansile intradural sausage-shaped lesion opposite L3–L4 vertebrae at the level of filum terminale [Figure 1]. The lesion showed mild diffusion restriction and intense postcontrast enhancement [Figure 2]. There was another similar smaller intradural lesion at the level of S2–S3 level. The lesion characteristics most likely represented a neoplastic etiology with drop metastasis. The patient then underwent durotomy and punch biopsy from the spinal lesion. Histopathology report showed cuboidal to elongated cells arranged radially around hyalinized fibrovascular cores in a capillary configuration with abundant myxoid stroma and areas of calcification and hemorrhage within features favoring myxopapillary ependymoma. Later, the patient underwent surgery and excision biopsy which reconfirmed the diagnosis of myxopapillary ependymoma. For further metastatic workup, he was advised to take an MRI brain to rule out the possibility of any brain metastasis. MRI brain showed extensive sulcal blooming in the bilateral cerebellum and bilateral cerebral hemispheres in the susceptibility-weighted

Access this article online

Quick Response Code:

Website: https://journals.lww.com/hrcm/

DOI: 10.4103/JHCR.JHCR_15_24

Address for correspondence: Dr. D. I. Devikrishna, Department of Radiodiagnosis, Amala Institute of Medical Sciences, Thrissur - 680 555, Kerala, India.
E-mail: devikrishnadi21@gmail.com

Received: 07-07-2024 **Revised:** 10-04-2025
Accepted: 11-04-2025 **Published:** ***

How to cite this article: Devikrishna DI, Joseph J, Ambooken RP, John SC. Superficial siderosis of the central nervous system secondary to spinal myxopapillary. J Adv Health Res Clin Med 2025;XX:XX-XX.

angiography sequences – suggestive of SS [Figure 3]. T2 fluid-attenuated inversion recovery images showed no obvious altered signal intensity in the sulcal spaces where blooming was present-consistent with the diagnosis of SS and differentiating it with acute subarachnoid hemorrhage [Figure 4].

SS was an incidental finding in this patient, who did not have any kind of neurological manifestations. On retrospective correlation, the most probable cause for SS in this patient was concluded to be myxopapillary ependymoma, as myxopapillary ependymoma was notorious in causing recurrent subarachnoid hemorrhages. The patient underwent microdecompression followed by placement of vertebral stabilization prosthesis. He was lost to follow-up.

Discussion

SS is a rare disorder arising secondary to chronic occult hemorrhages into the meninges of the central nervous system, although the primary cause of bleeding is seldom identified in the majority of cases by imaging. The common causes of recurrent subarachnoid hemorrhage and SS are spinal dural defects, intracranial neoplasms such as ependymoma and oligodendrogliomas, vascular abnormalities such as arteriovenous malformation and aneurysms and cerebral amyloid angiopathy. In a vast majority of cases, imaging fails to find a definite cause of SS and hence is labeled as idiopathic.[3]

The RBCs released into the subarachnoid space undergo hemolysis and release free iron. Free iron is highly reactive and releases toxic free radicals which cause lipid peroxidation, protein oxidation, and DNA damage, leading to chronic neuroinflammation and neuronal death.[4] It eventually causes neurological dysfunction, the classic manifestations being gradually progressive ataxia, dysarthria, and hearing loss (sensorineural type).[2,5] The development of symptoms occurs after many years of disease onset and is often insidious.

Routine MRI of the brain is the ideal investigation modality for the detection of SS.[6] MR images classically show areas of decreased signal intensity surrounding and layering the periphery of the brain, particularly noted with the gradient echo or SWAN sequences.[7] The treatment strategy of SS is basically early detection of the site of bleeding and opting for appropriate surgical correction.

In our patient, myxopapillary ependymoma of the spinal cord was identified as the source of bleeding which led to the development of SS. Myxopapillary ependymomas are variant forms, different from classical spinal ependymoma in a way that it arises from the terminal end of the spinal cord, namely the conus medullaris and filum terminale. In MRI, they appear as T1 isointense and T2 hyperintense lesion with homogenous postcontrast enhancement. Histologically, they contain variable

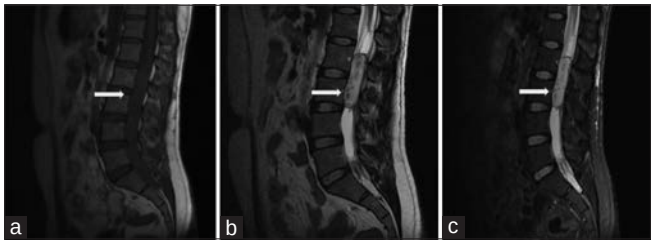

Figure 1: MRI Sagittal T1 (a), T2 (b), and STIR (c), images of the lumbar spine depicting, a T1 hypointense (arrow in fig a), T2 and STIR hyperintense (arrow in fig b and c), expansile intradural sausage shaped lesion opposite L3-L4 vertebrae at the level of filum terminale consistent with diagnosis of myxopapillary ependymoma

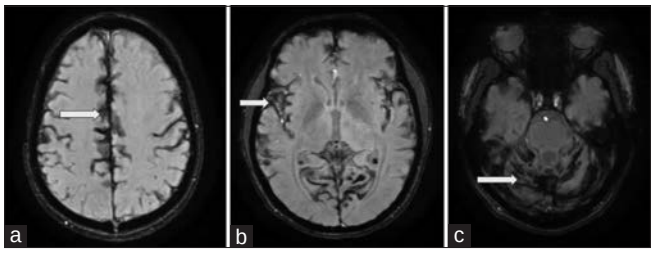

Figure 3: MRI brain - Axial susceptibility weighted angiography sequence depicting extensive sulcal blooming in bilateral cerebral hemispheres and cerebellum(arrows in fig a, b, and c) - suggestive of superficial siderosis

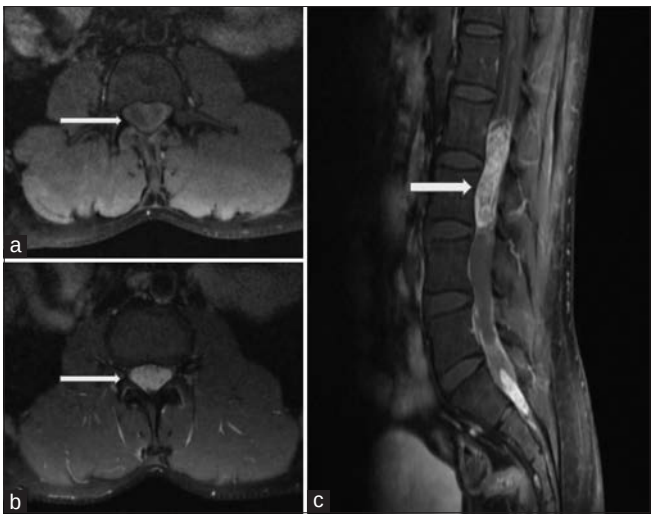

Figure 2: MRI Lumbar spine - Axial (a and b) and Sagittal (c) T1 post contrast images depicting intense heterogenous post contrast enhancement of the lesion (arrows in fig a, b and c) with evidence of drop metastasis

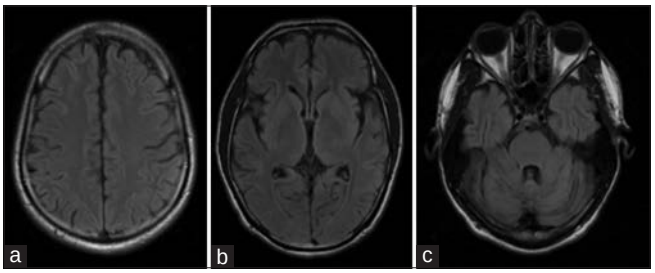

Figure 4: Magnetic resonance imaging brain T2 fluid-attenuated inversion recovery images depicting no significant altered signal intensities in the sulcal spaces of brain parenchyma - consistent with the diagnosis of superficial siderosis

papillary architecture, with cells arranged radially around a fibrovascular core with perivascular myxoid changes, forming pseudorosettes. They are glial fibrillary acidic protein, S100, and vimentin-positive in immunophenotyping.[8]

Since the treatment of SS is early detection and correction of the bleeding source,[9] neurosurgical intervention of spinal myxopapillary ependymoma was considered an effective therapy.

Conclusion

This case report concluded that incidental diagnosis of SS in a young adult and on retrospective correlation, myxopapillary ependymoma was identified as the most probable cause for the same. The SS may be clinically silent and in such cases, MRI of the brain and spine is needed for deciding the appropriate choice of management.

Declaration of patient consent

The authors certify that they have obtained all appropriate patient consent forms. The patient understands that his name and initials will not be published and due efforts will be made to conceal his identity, but anonymity cannot be guaranteed.

Financial support and sponsorship

Nil.

Conflicts of interest

There are no conflicts of interest.

References

1. Rodriguez FR, Srinivasan A. Superficial siderosis of the CNS. Am J Roentgenol 2011;197:W149-52.
2. Kumar N. Neuroimaging in superficial siderosis: An in-depth look. Am J Neuroradiol 2010;31:5-14.
3. Weerakkody Y. Radiopaedia. . Superficial siderosis of the central nervous system | Radiology Reference Article | Available from: https://Radiopaedia.org. [Last accessed on 2024 Dec 10].
4. Superficial Siderosis. National Organization for Rare Disorders. Available from: https://rarediseases.org/rare-diseases/superficial-siderosis/?utm_source=chatgpt.com. [Last accessed on 2025 Mar 22].
5. Khalatbari K. "Case 141: Superficial Siderosis." Radiology, vol. 250, no. 1; 2009. p. 292–7. [doi: org/10.1148/radiol.2501051201].
6. Harizi E, Shemsi K, Ahmetgjekaj I, Parisapogu A, Mamillo K, Hyseni F, *et al.* Superficial intraventricular surface siderosis brain. Radiol Case Rep 2022;17:4152-5.
7. Superficial Siderosis. Available from: https://Appliedradiology.com. [Last accessed on 2024 Jul 20].
8. Nair S, Rudrabhatla P, Sabarish S, George T, Divakar G, Sylaja PN. Superficial siderosis due to spinal myxopapillary ependymoma mimicking idiopathic intracranial hypertension. Ann Indian Acad Neurol 2022;25:156-7.
9. Choi KE, Na SH, Jeong HS, Im JJ, Kim YD. Superficial siderosis of the central nervous system due to spinal ependymoma. Ann Geriatr Med Res 2018;22:43-5.